



Microwave-driven breakdown: from dielectric surface multipactor to ionization discharge[†]

J. P. Verboncoeur¹, J. Booske², R. Gilgenbach³, Y. Y. Lau³, A. Neuber⁴, J. Scharer², R. Temkin⁵

¹Michigan State University/University of California-Berkeley, ²University of Wisconsin, ³University of Michigan, ⁴Texas Tech University, ⁵Massachussets Institute of Technology

† Research supported by an AFOSR grant on the Basic Physics of Distributed Plasma Discharges

Goals



- Understand basic physics of microwavedriven breakdown
 - Breakdown threshold dependence on pressure, gas composition, geometric features
 - Low Pressure Dielectric Multipactor
 - Transition to Ionization Discharge
 - Compare Experiments and Theory





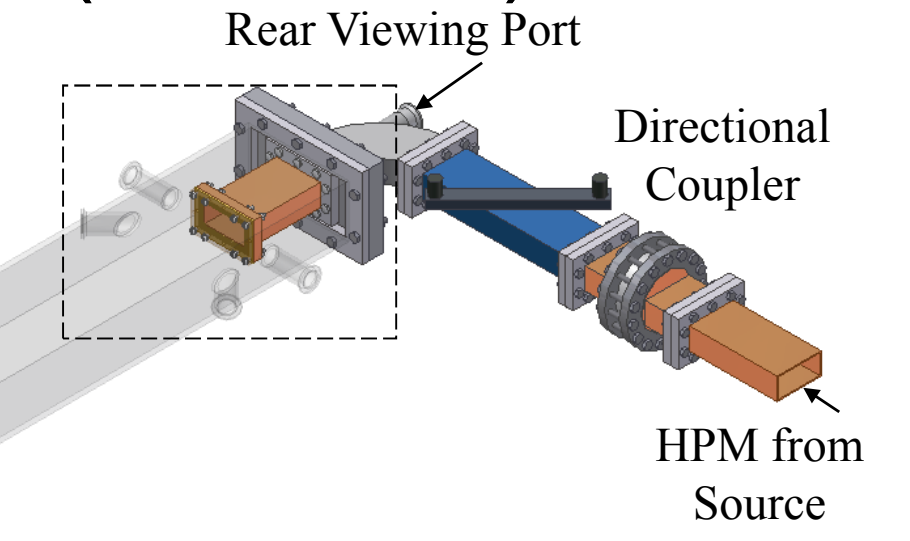
Experimental Setup (2.85 GHz)

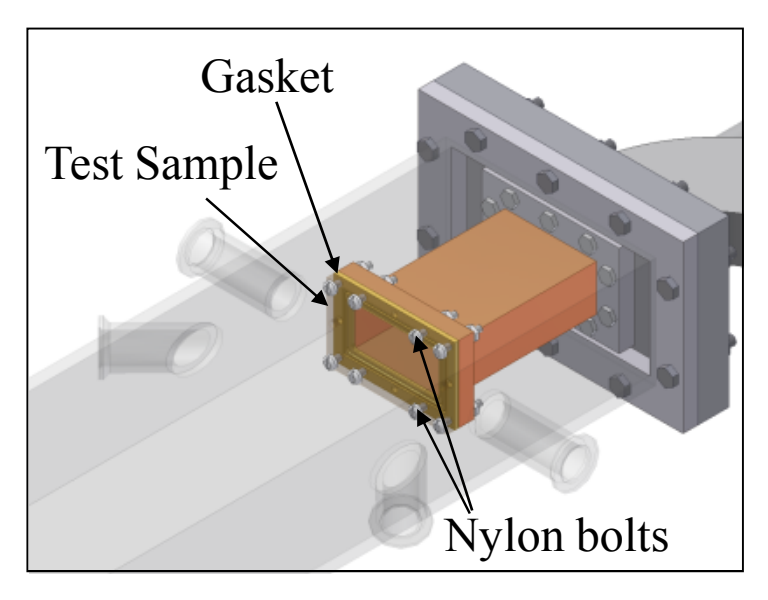
HPM Load Directional Coupler Front Viewing Port

Test Section

Test Section Features

- •WR284-WR650 Standards
- •Not optimized for transmission (Simple geometry to study effects)
- •High-loss silicone rubber sheets
- •Side and 45° Viewing Ports
- Atmospheric Control

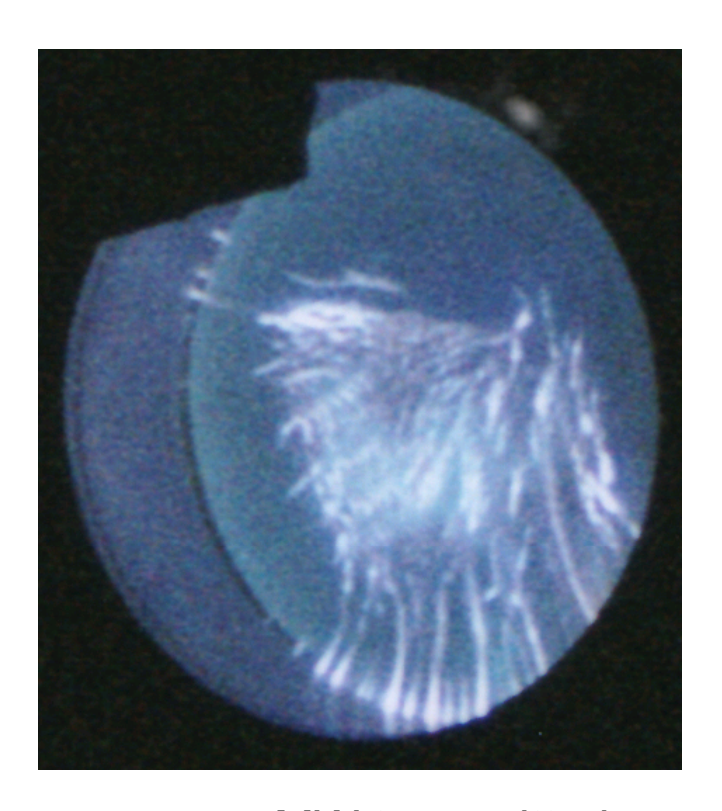


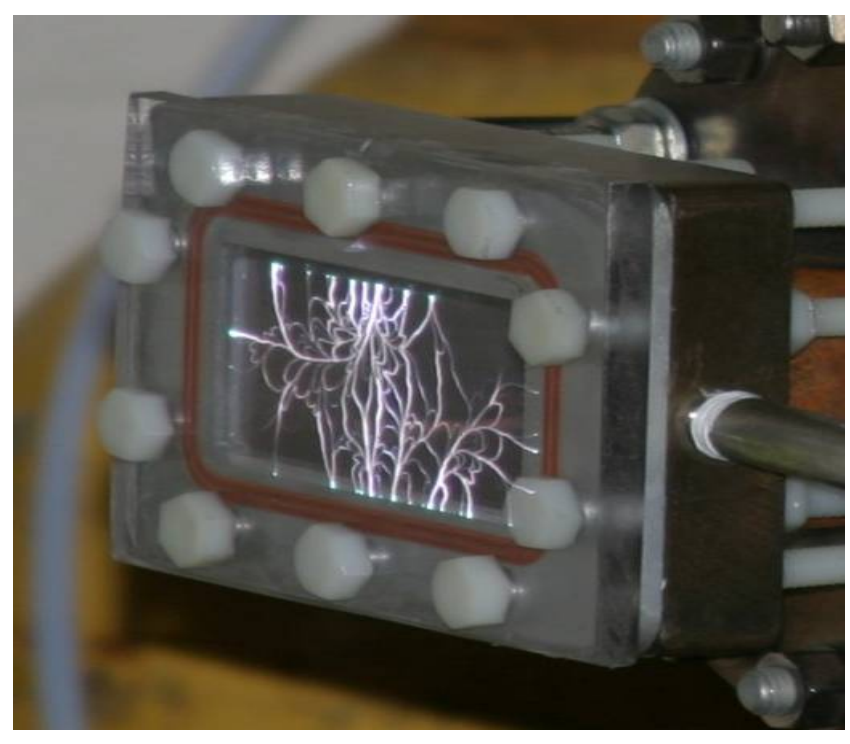




RF Window Flashover







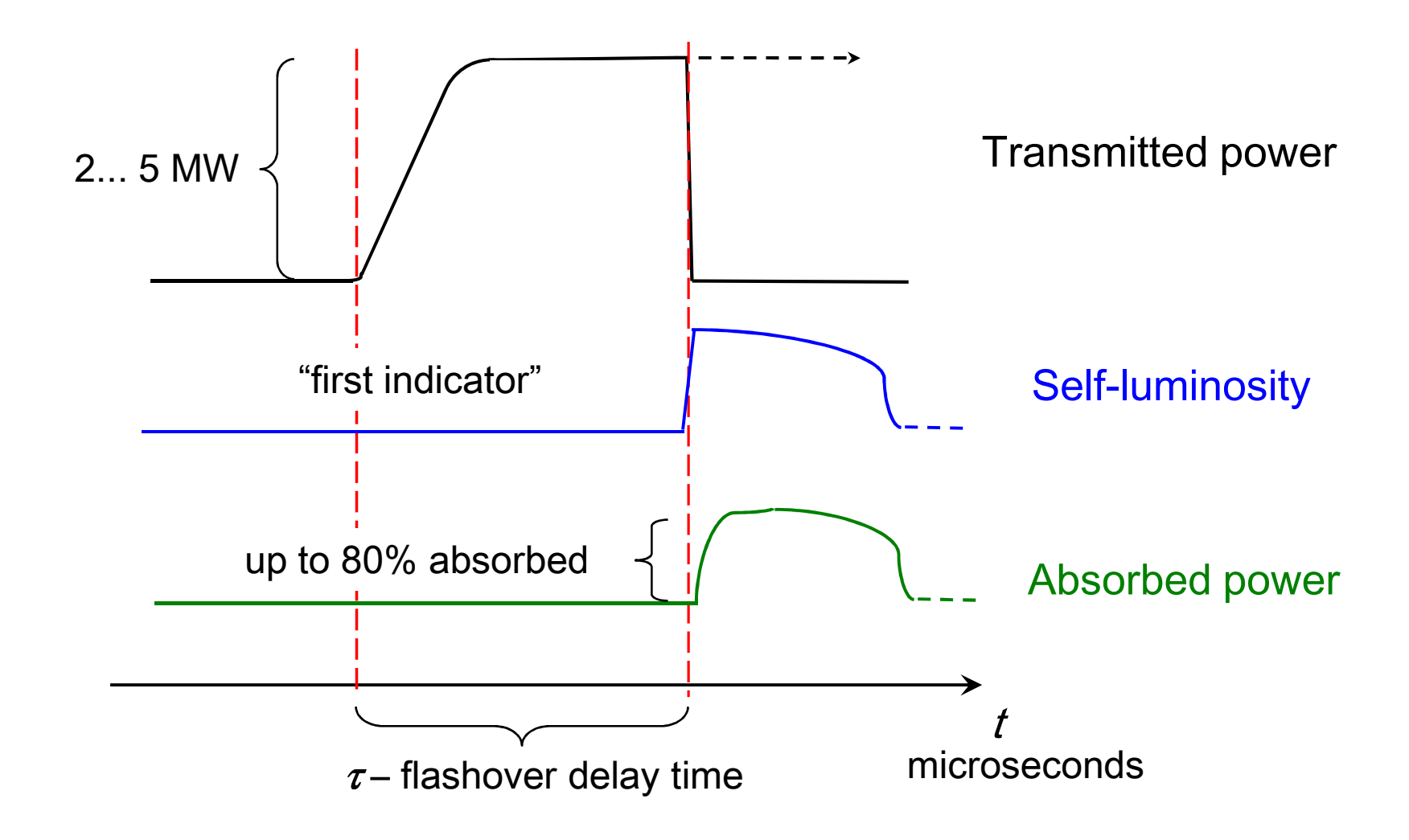
- > MW transmitted power (High Power Microwaves, HPM)
- → Field amplitudes in excess of several 10 kV/cm

Flashover can be initiated with or without the presence of a triple point



Observed Waveforms

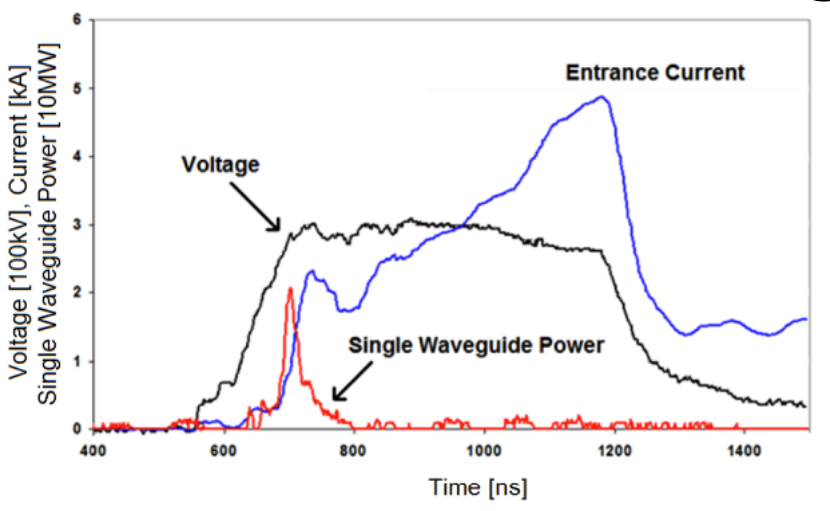


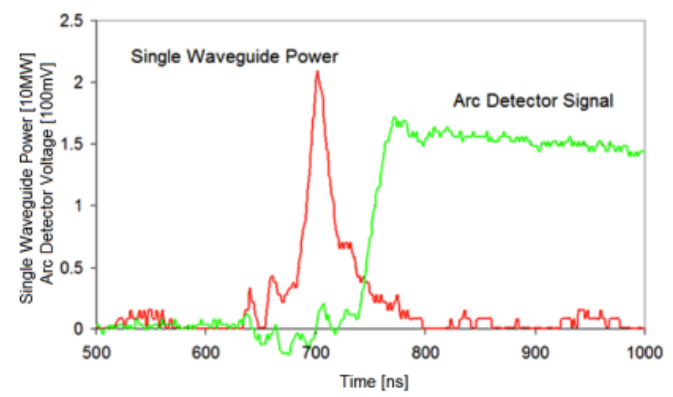


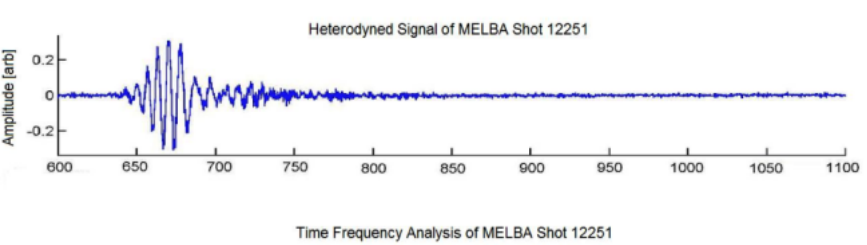


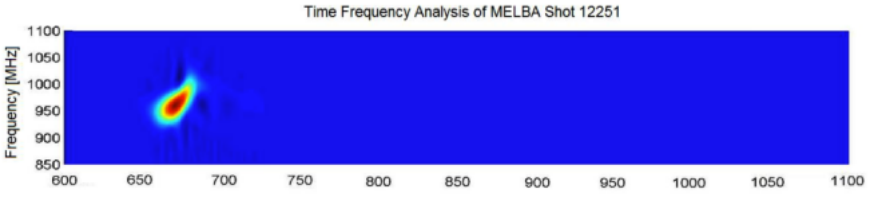
UM RelMag: old window

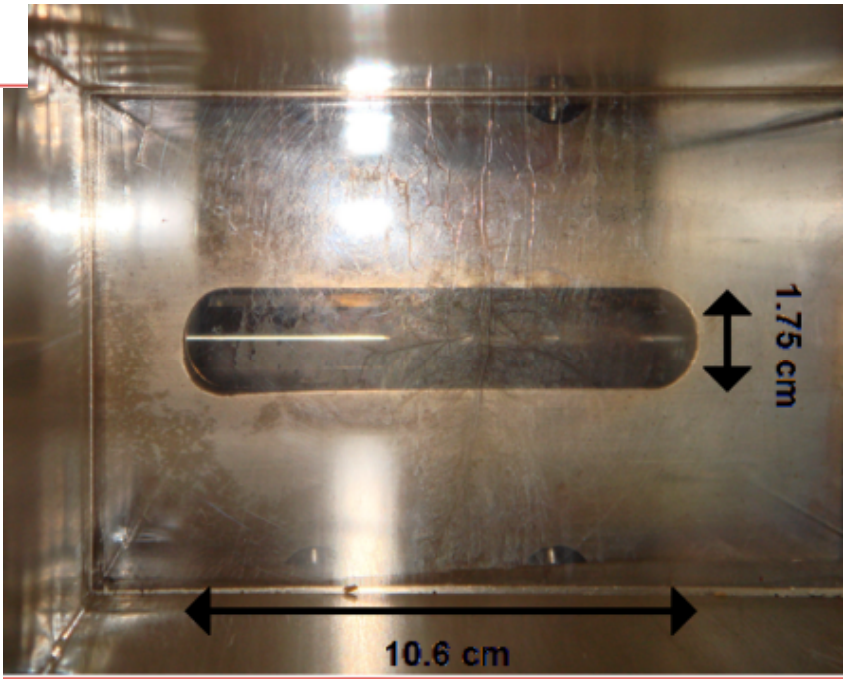






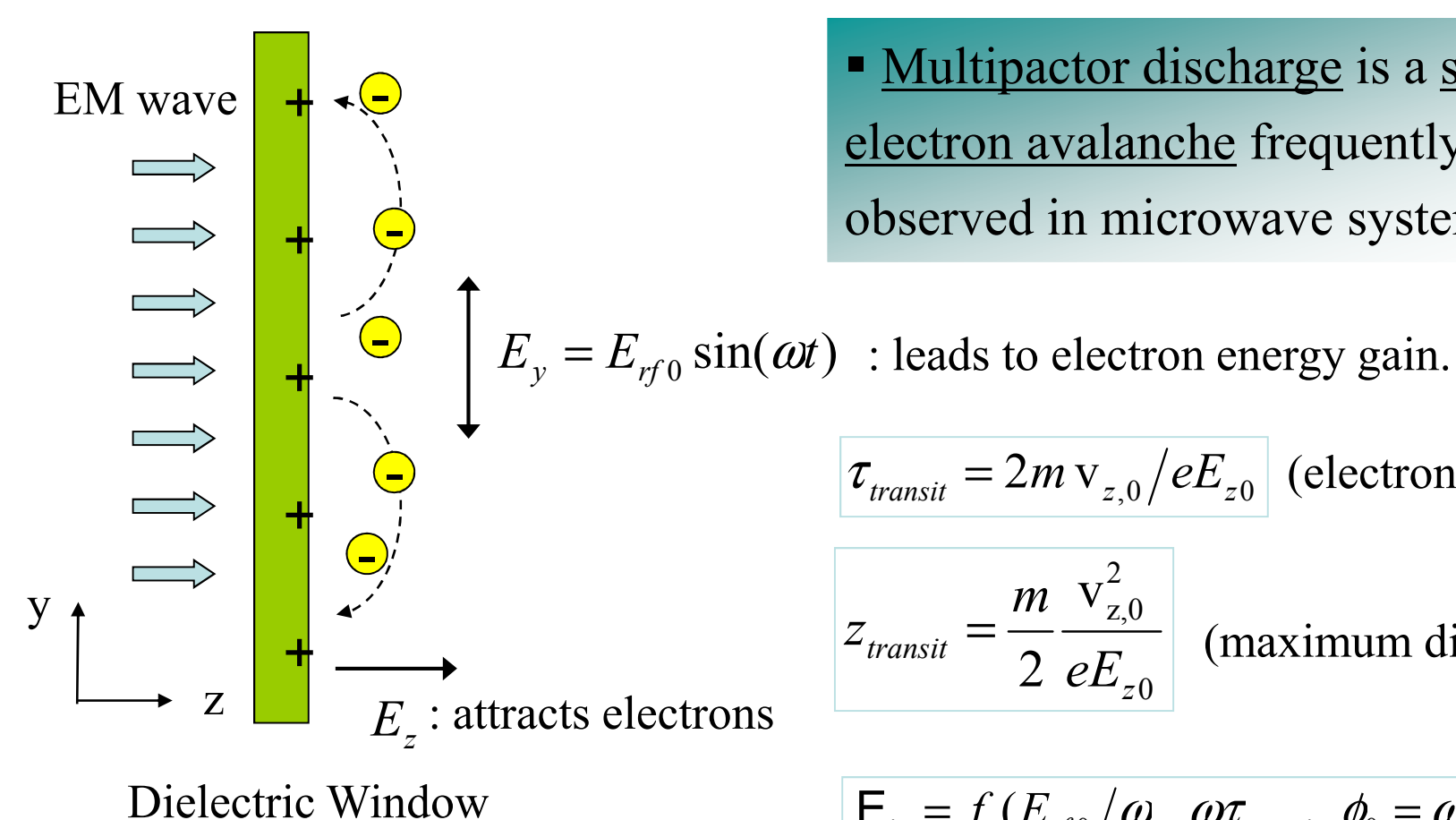






Single-Surface RF Multipactor





Multipactor discharge is a secondary electron avalanche frequently observed in microwave systems.

$$\tau_{transit} = 2m \, v_{z,0} / eE_{z0}$$
 (electron life time)

$$z_{transit} = \frac{m}{2} \frac{\mathbf{v}_{z,0}^2}{eE_{z0}}$$
 (maximum distance)

$$\mathsf{E}_{iy} = f\left(E_{rf0}/\omega, \ \omega \tau_{transit}, \phi_0 = \omega t_0\right)$$

Secondary Electron Model



Energy and angular dependence of secondary emission coefficient

$$\delta(E_{i},\theta) = \delta_{\max 0} (1 + \frac{k_{s\delta}\theta^{2}}{2\pi}) \begin{cases} (we^{1-w})^{k}, & w \leq 3.6 \\ \frac{1.125}{w^{0.35}}, & w > 3.6 \end{cases}$$

$$k = \begin{cases} 0.56, & w < 1 \\ 0.25, & 1 \leq w \leq 3.6 \end{cases}$$

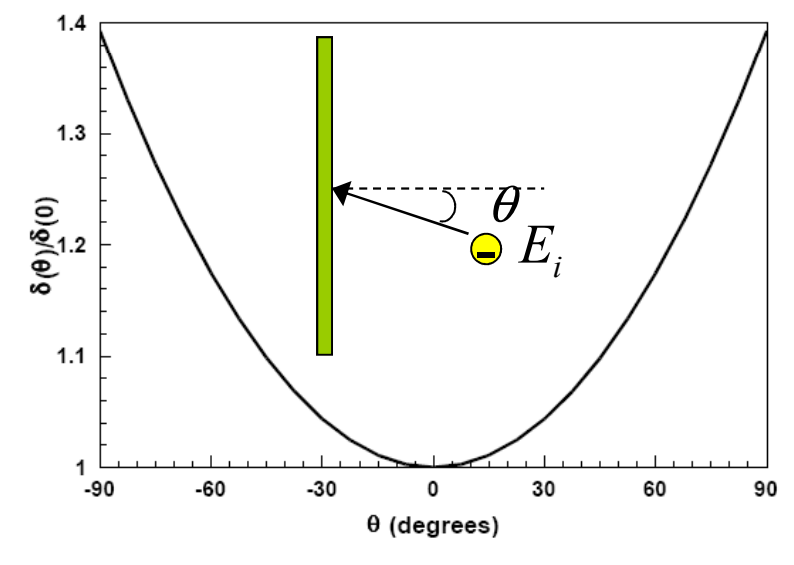
$$E_{i} \text{ (Electron Impact Energy)}$$

 $\delta > 1$

 δ < 1

$$w = \frac{E_i - E_0}{E_{\text{max}0} (1 + k_{sw} \theta^2 / 2\pi) - E_0}$$

$$k = \begin{cases} 0.56, & w < 1 \\ 0.25, & 1 \le w \le 3.6 \end{cases}$$

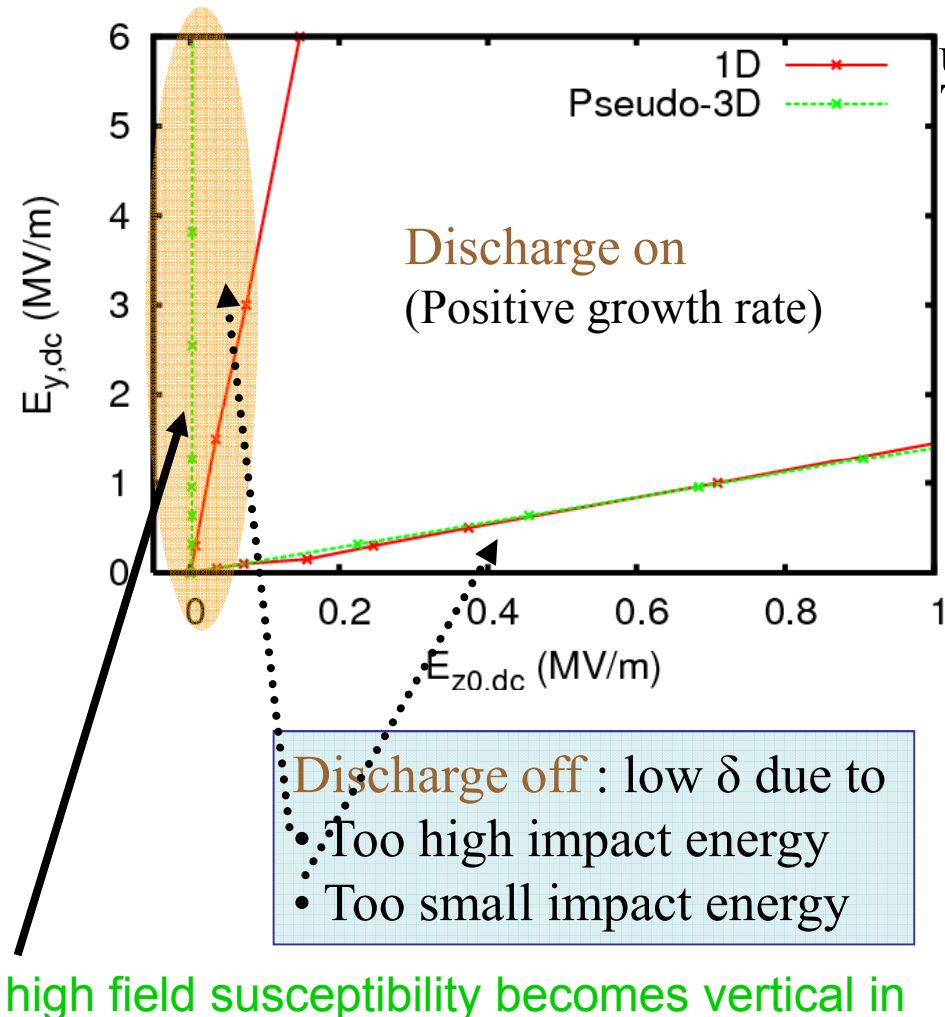


θ (Electron Impact Angle)

 δ < 1

PIC Multipactor Susceptibility

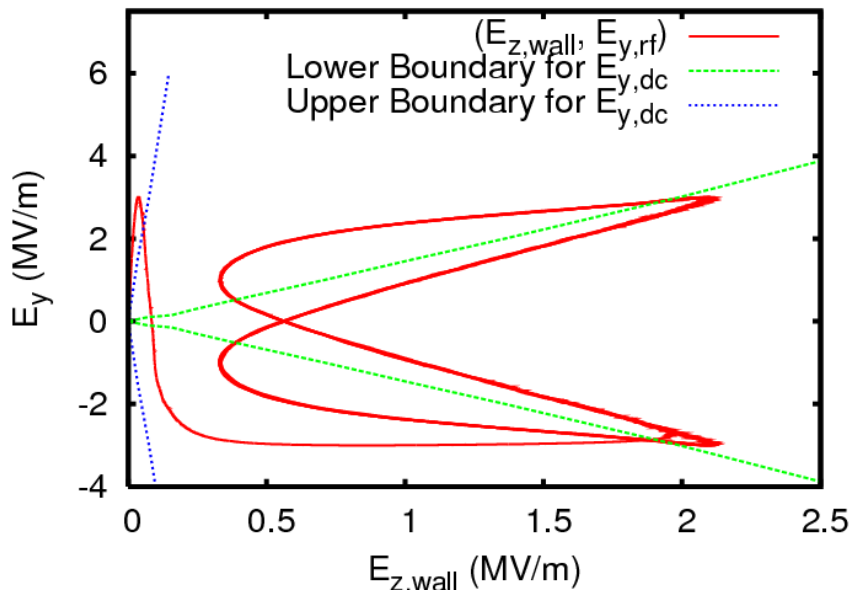




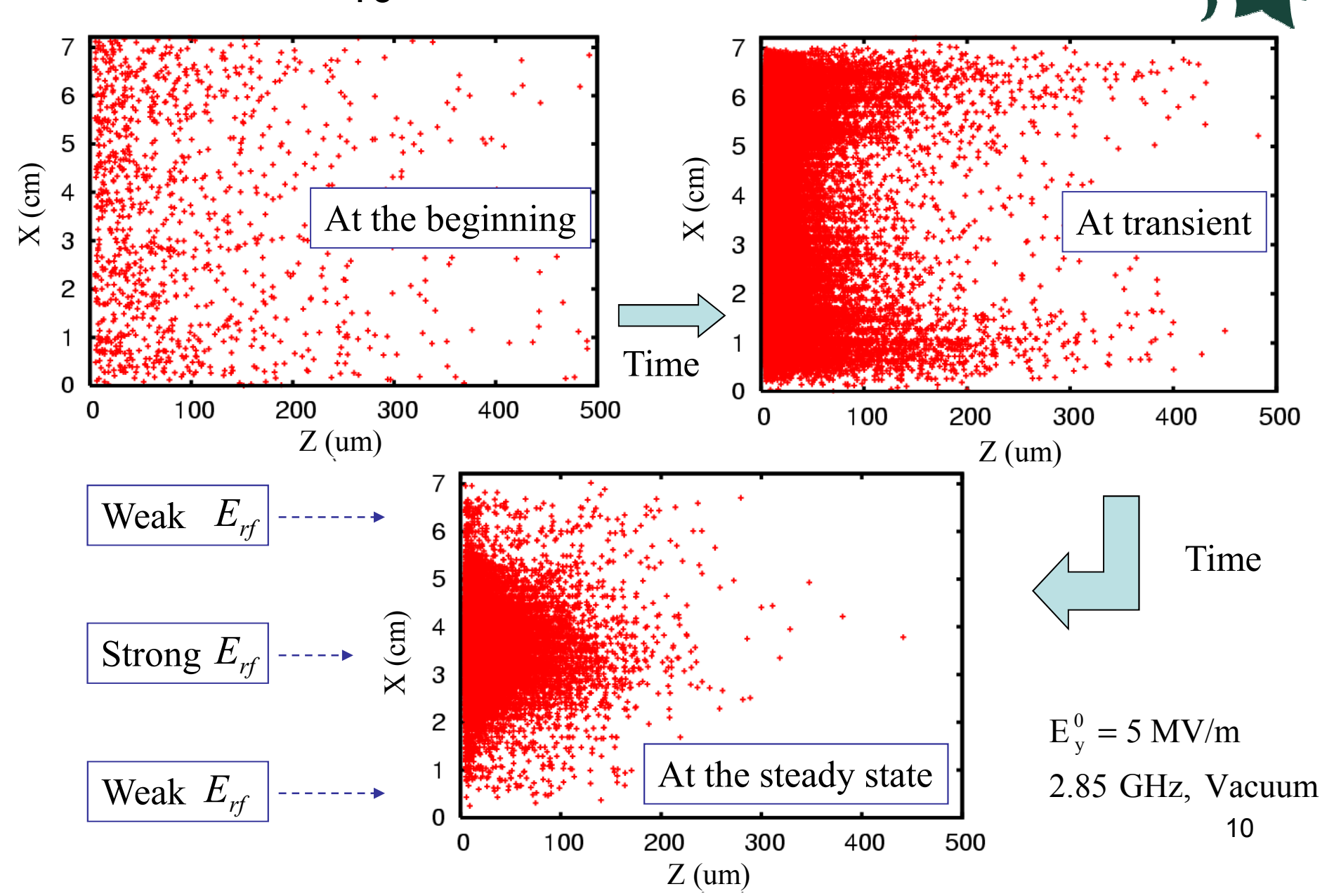
waveguide – no upper field cutoff

uniform plane wave TE10 rectangular waveguide

- include transverse variation of E_{RF}
- absorb at transverse wall
- neglect transverse space charge



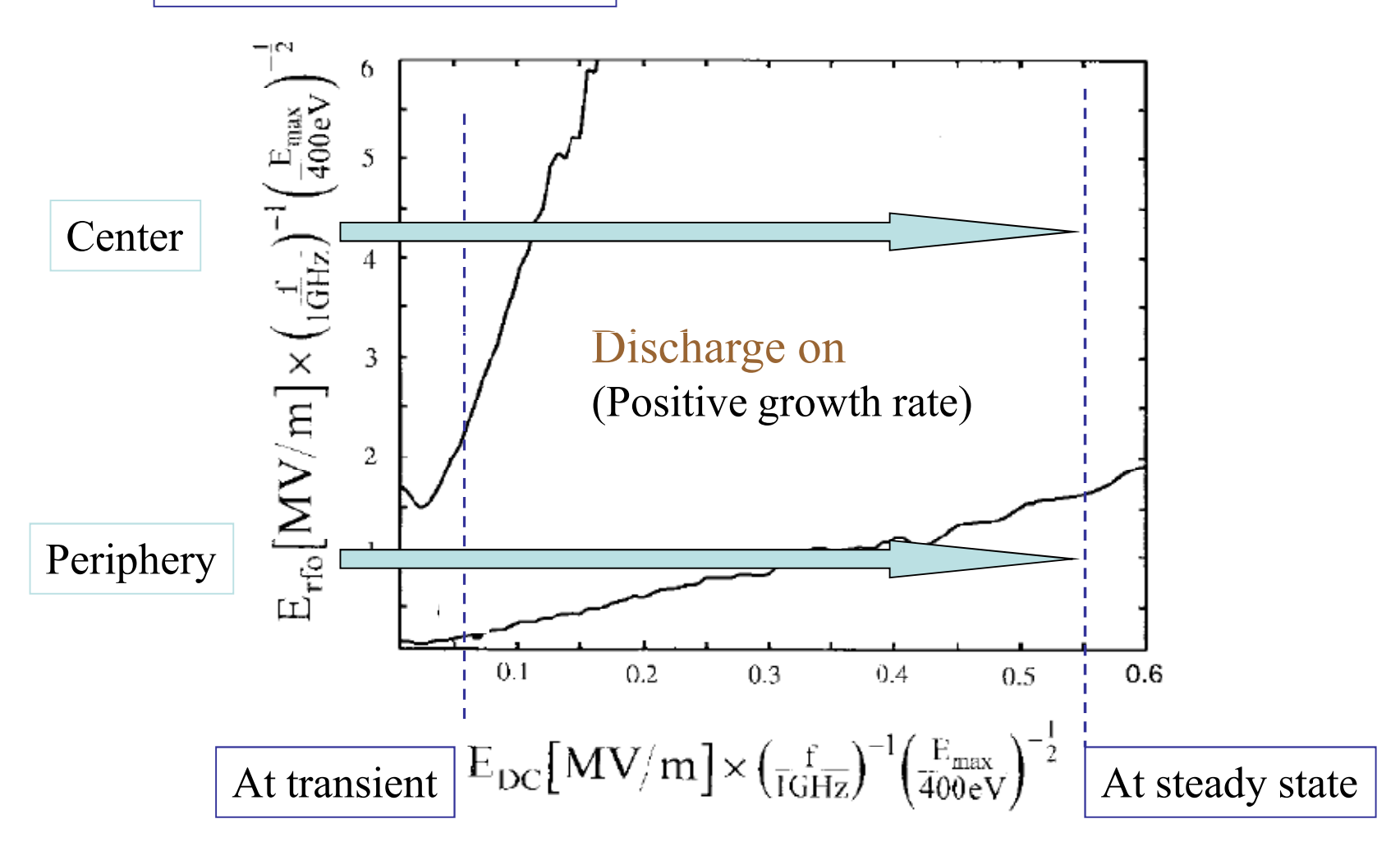
TE₁₀ Multipactor Migration



Explanation of Migration

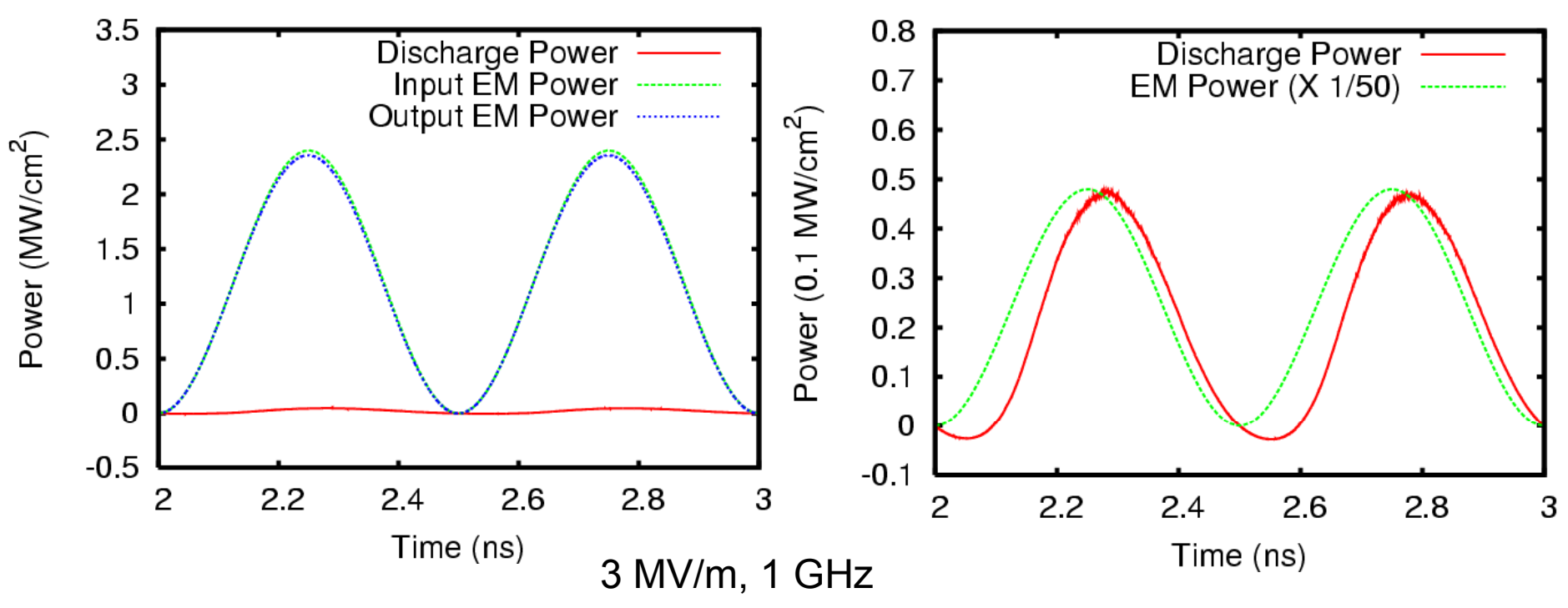


Susceptibility Curve



Multipactor Power

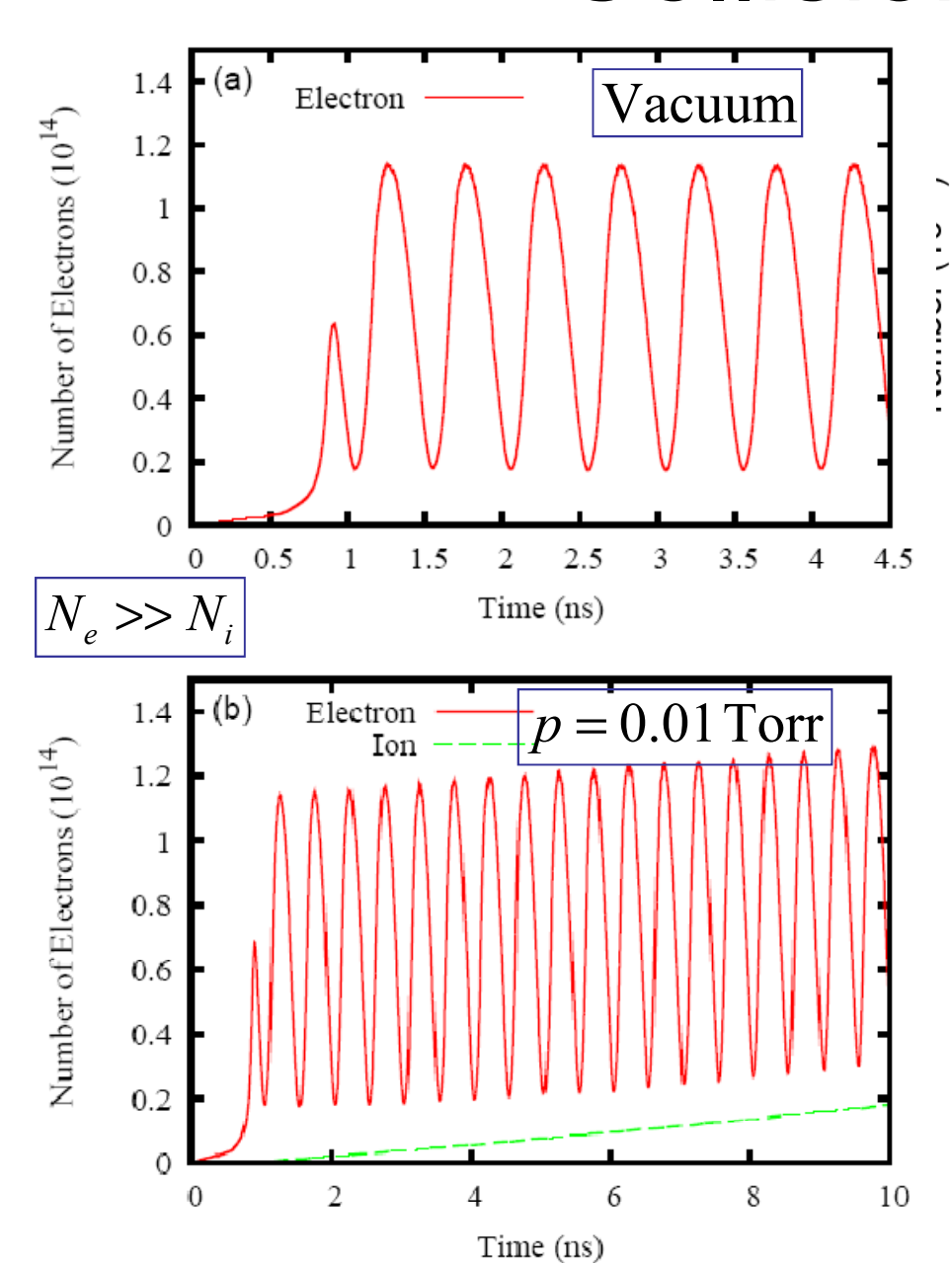


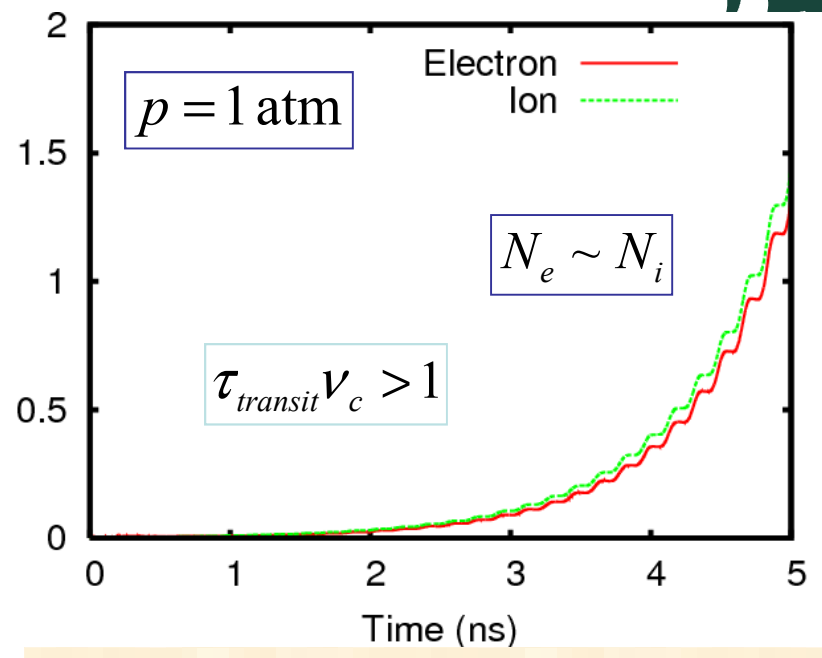


- ~2 % of the input EM power is absorbed
- The phase difference between the discharge power and input EM power means that the electrons are not totally in equilibrium with the local rf electric field.

Collisional Effects





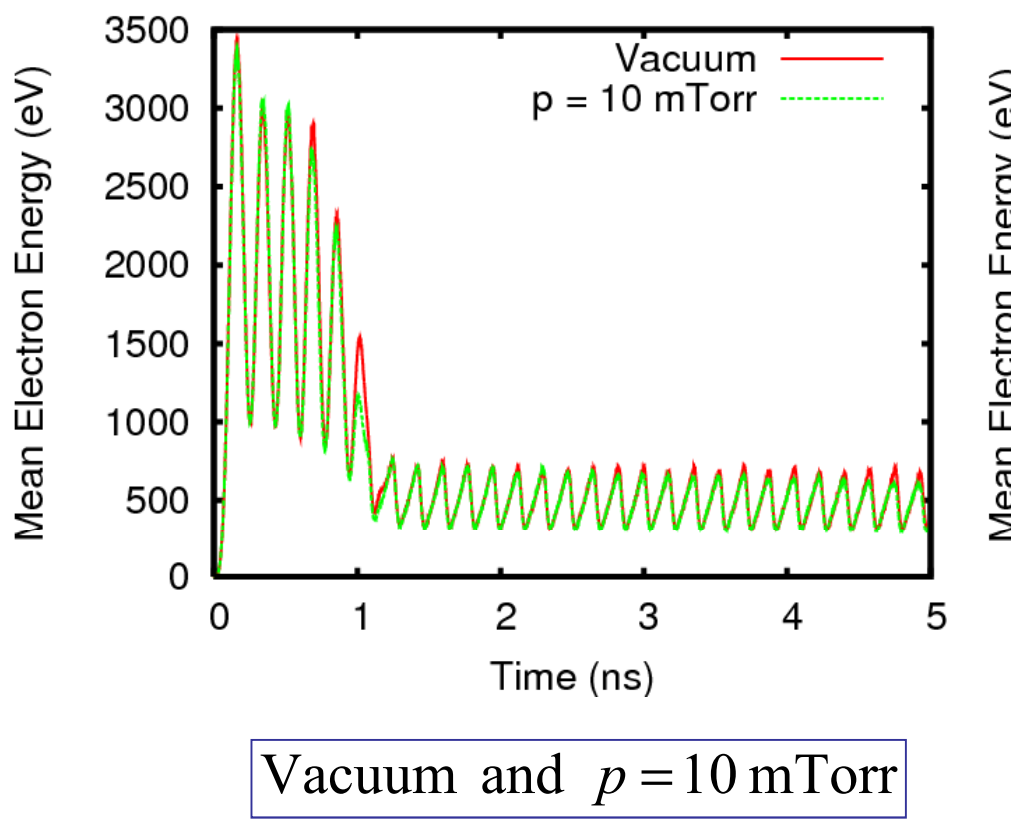


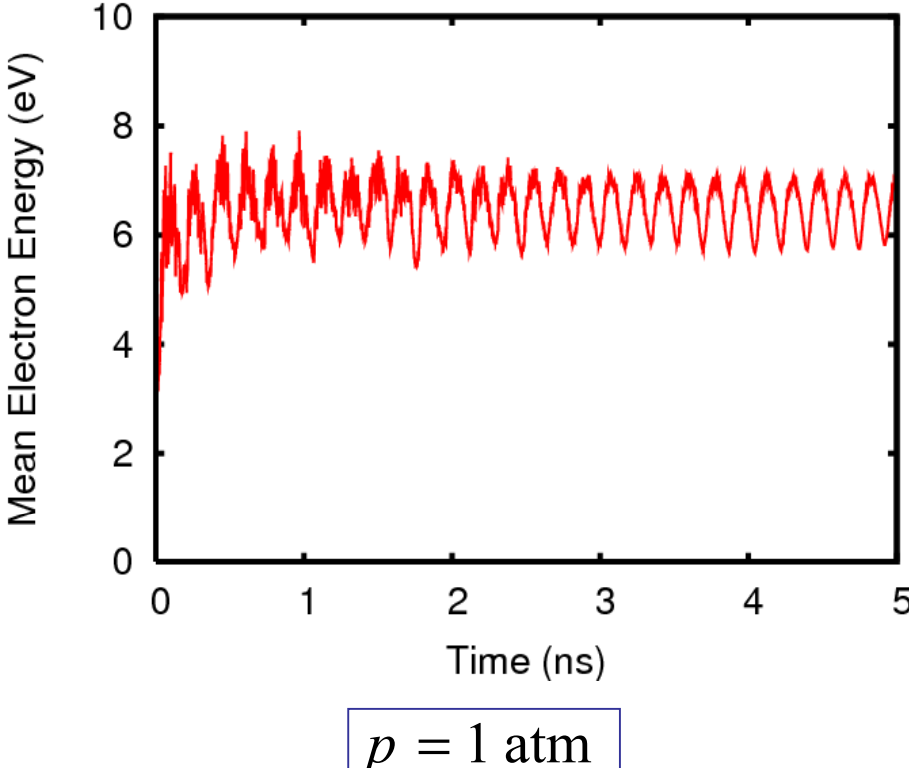
- As the pressure increases, electronimpact ionization collisions dominate secondary electron emission as the electron source.
- At high pressures, the number of ions becomes comparable to that of electrons.

$$E_{rf0} = 3 \text{ MV/m} \text{ at } 1 \text{ GHz, Argon}$$
 13

PIC: Electron Mean Energy





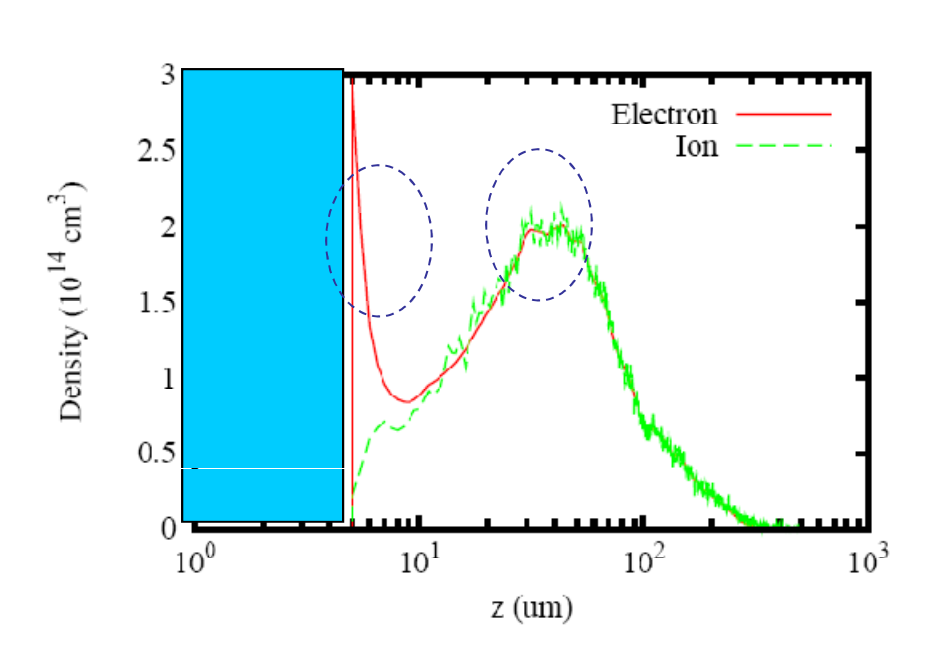


• Electrons in the multipactor discharge gain their energy by being accelerated by the rf electric field during the transit time.

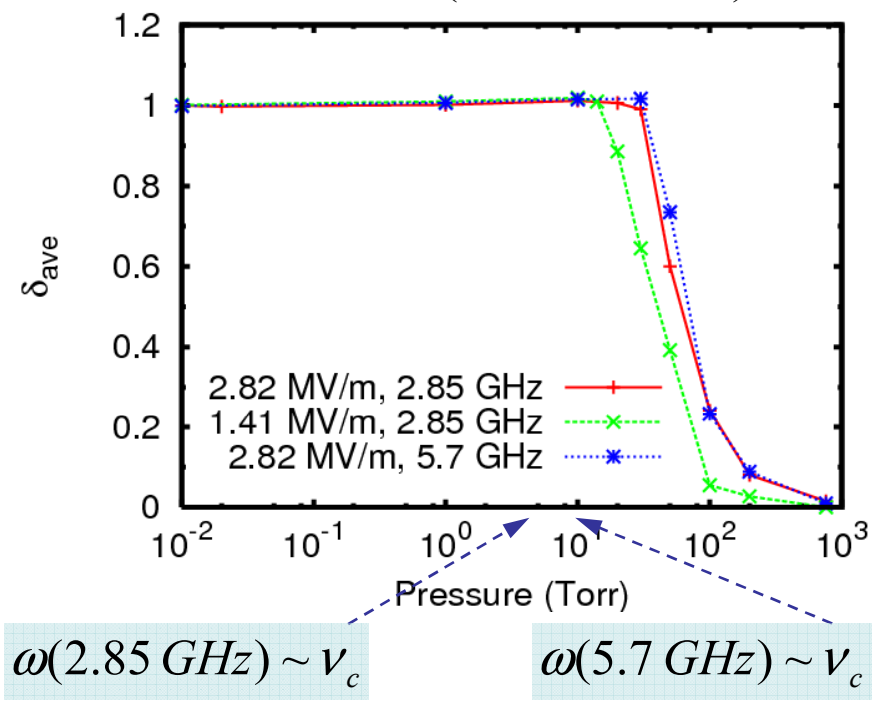
• At high pressures, electrons <u>suffer</u> many collisions and lose a significant amount of energy gained from the rf electric field.

Transition





Transition Pressure (10~50 Torr Ar)

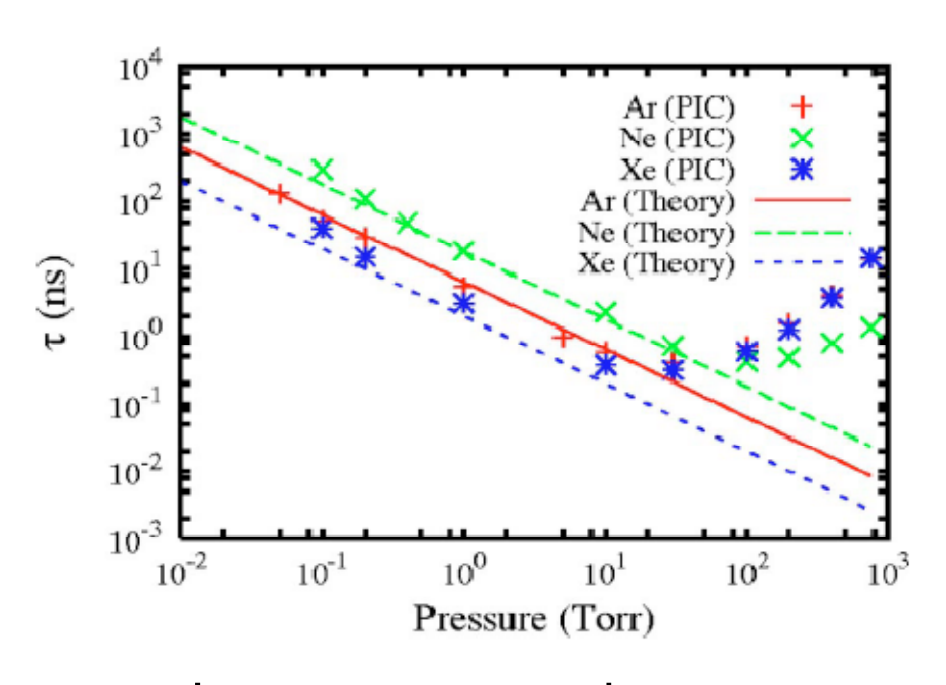


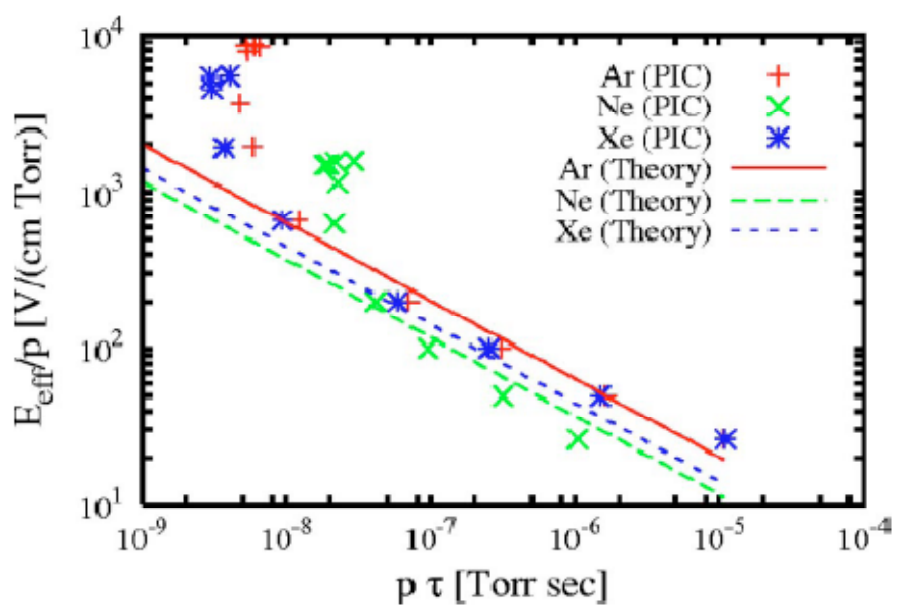
1 Torr: surface and volume discharges coexist

- Below 10 Torr, the secondary yield is nearly unity so multipactor is dominant.
- As the pressure increases and hence the volume discharge suppresses the secondary electron emission, it decreases to nearly zero.

Breakdown Scaling Law







Low pressure regime: surface multipactor dominated

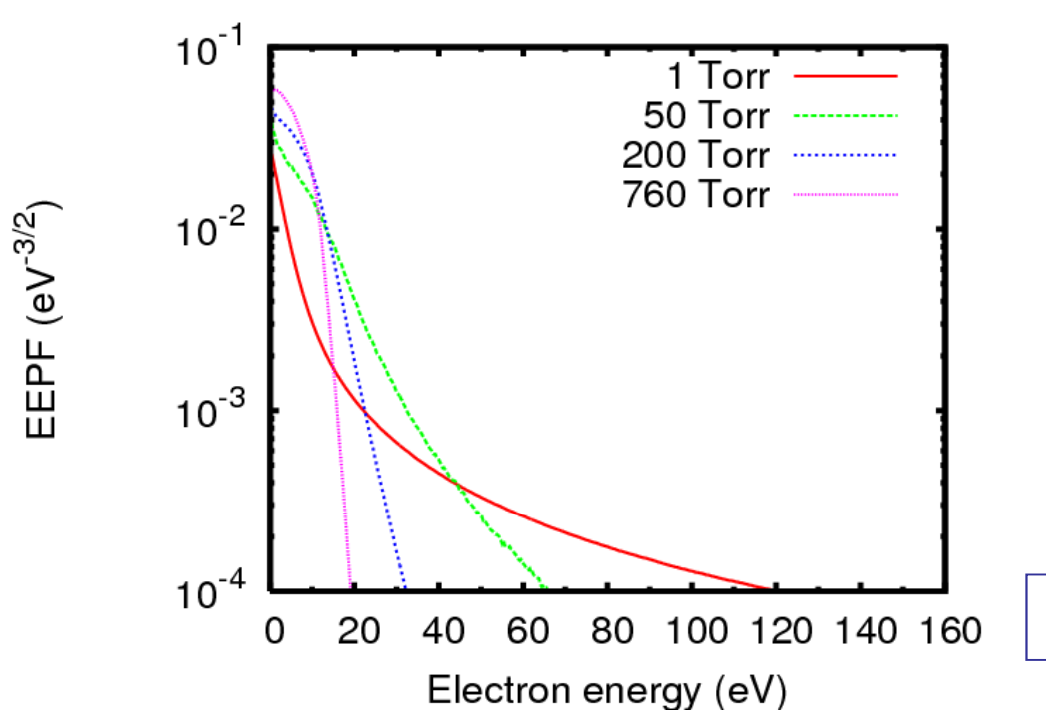
$$au \sim \frac{1}{v_i} \sim \frac{1}{n_g \langle \sigma v \rangle} \sim \frac{1}{p}$$

High pressure regime: collision dominated ($v_c >> \omega$) volumetric discharge

$$rac{E_{\mathit{eff}}}{p} \sim rac{1}{\sqrt{p\, au}}$$

PIC: Electron Energy Distribution



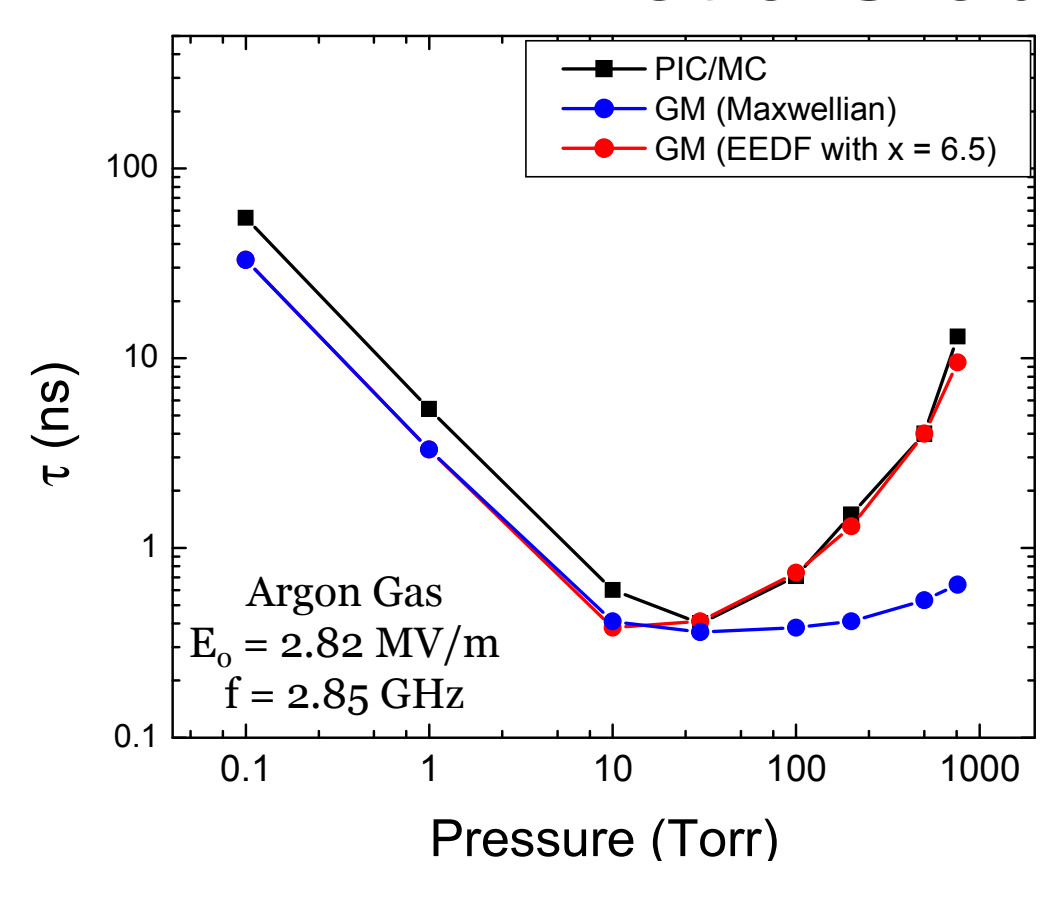


Spatially averaged

- Below 50 Torr, the EEPF is bi-Maxwellian like
- At high pressures, the EEPF becomes cutoff, with the depletion of high-energy electrons $v_c > \omega$

Kinetic Global Model





Assume general distribution function:

$$f(\varepsilon) = c_1 \varepsilon^{1/2} e^{-c_2 \varepsilon^x}$$

Solve continuity, energy, and power absorption equations for each species

Get x for distribution function from PIC: Good over 4 orders in pressure!

Works for all gases tried – shape depends only on cross sections

From PIC:
$$K_{ion}|_{PIC} = \int_{\varepsilon_{ion}} \sqrt{\frac{2e\varepsilon}{m_e}} \cdot \sigma_{ion}(\varepsilon) \cdot c_1 \varepsilon^{1/2} e^{-c_2 \varepsilon^x} d\varepsilon$$
 (Ar)

Kinetic Global Model* II



 Coupled continuity equations for all species, e.g. for oxygen:

$$\begin{split} \frac{dn_{e}}{dt} &= K_{ion}n_{e}n_{gas} - K_{att}n_{e}n_{gas} - K_{rec}n_{e}n_{O_{2}^{+}} + K_{\det}n_{e}n_{O^{-}} + K_{\det2}n_{O_{2}^{+}}n_{O^{-}} \\ \frac{dn_{O_{2}^{+}}}{dt} &= K_{ion}n_{e}n_{gas} - K_{rec}n_{e}n_{O_{2}^{+}} - K_{mut}n_{O^{-}}n_{O_{2}^{+}} \\ \frac{dn_{O^{-}}}{dt} &= K_{att}n_{e}n_{gas} - K_{\det}n_{e}n_{O^{-}} - K_{mut}n_{O^{-}}n_{O_{2}^{+}} - K_{\det2}n_{O_{2}^{+}}n_{O^{-}} \end{split}$$
 where
$$K = \int \sqrt{\frac{2e\varepsilon}{C}} \sigma(\varepsilon) f(\varepsilon) d\varepsilon$$

where
$$K = \int_{\varepsilon} \sqrt{\frac{2e\varepsilon}{m_e}} \sigma(\varepsilon) f(\varepsilon) d\varepsilon$$

Oxygen Reactions



$$1)e+O_2 \rightarrow e+O_2$$

$$2)e + O_2 \rightarrow e + O_2(r)$$

$$3-6)e+O_2 \rightarrow e+O_2(v=n, n=1,2,3,4)$$

$$7)e+O_2 \rightarrow e+O_2(a^1\Delta_g)$$

$$8)e+O_2 \rightarrow e+O_2(b^1\Sigma_g^+)$$

$$9)e+O_2 \rightarrow O+O^-$$

$$10)e+O_2 \rightarrow e+O_2(c^1\Sigma_u^-, A^3\Sigma_u^+)$$

11)
$$e+O_2 \rightarrow e+O(3P)+O(3P)$$

$$12)e + O_2 \rightarrow e + O(3P) + O(1D)$$

13)
$$e + O_2 \rightarrow e + O(1D) + O(1D)$$

$$14)e + O_2 \rightarrow e + O_2^+ + e$$

$$15)e+O_2 \to e+O+O^*(3p^3P)$$

$$16)e+O_2^+ \to O+O$$

$$17)e+O^{-} \rightarrow e+O+e$$

$$(18)O^{-} + O_{2}^{+} \rightarrow O + O_{2}$$

$$19)O^{-} + O_{2} \rightarrow O + O_{2} + e$$

Enhanced Global Model III



Electron energy equation:

$$\frac{d}{dt}\left(\frac{3}{2}n_{e}kT_{eff}\right) = P_{abs} - (\varepsilon_{ion}K_{ion}n_{e}n_{gas} + \sum_{exc}\varepsilon_{exc}K_{exc}n_{e}n_{gas} + \widetilde{K}_{mom}n_{e}n_{gas})$$

Improved RF power absorption model:

$$P_{abs} = \int \frac{e^2 n_e}{m v_m} \left(\frac{E_0}{\sqrt{2}} \frac{v_m}{\sqrt{v_m^2 + \omega^2}} \right)^2 f(\varepsilon) d\varepsilon$$

Enhanced Global Model IV



• The general EEDF equation in the isotropic velocity space *:

$$f(\varepsilon) = c_1 \varepsilon^{1/2} e^{-c_2 \varepsilon^x}$$

- Maxwellian: x=1, Druyvestyn: x=2
- Determine x by the ionization and dissociative attachment from PIC model:

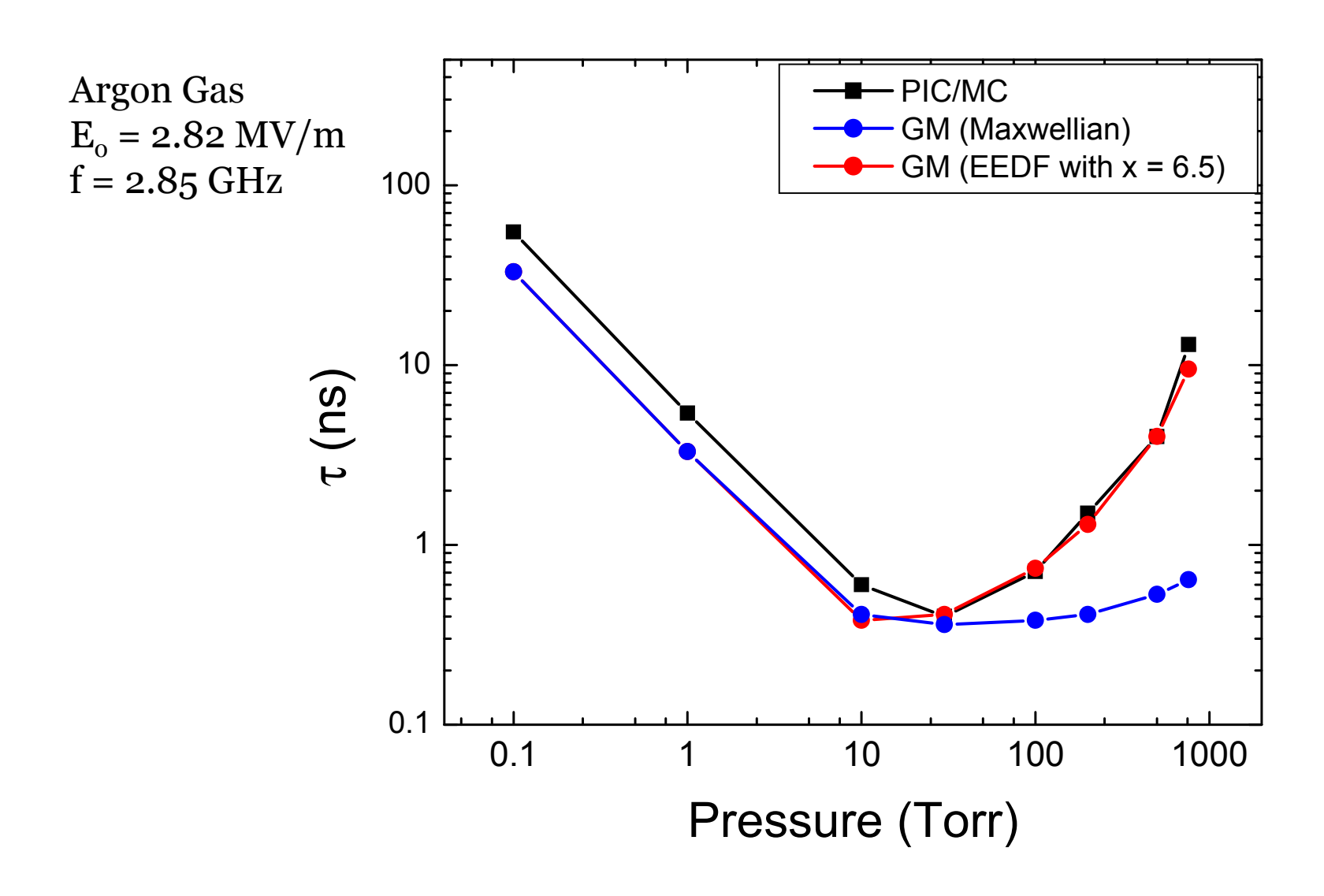
$$K_{ion}\big|_{PIC}$$
 - $K_{att}\big|_{PIC}$ =

$$\int_{\varepsilon_{\text{ion}}} \sqrt{\frac{2e\varepsilon}{m_e}} \cdot \sigma_{\text{ion}}(\varepsilon) \cdot c_1 \varepsilon^{1/2} e^{-c\left(\frac{\varepsilon}{T_{\text{eff}}}\right)^x} d\varepsilon - \int_{\varepsilon_{\text{att}}} \sqrt{\frac{2e\varepsilon}{m_e}} \cdot \sigma_{\text{att}}(\varepsilon) \cdot c_1 \varepsilon^{1/2} e^{-c\left(\frac{\varepsilon}{T_{\text{eff}}}\right)^x} d\varepsilon$$

* J. T. Gudmundsson, Plasma Sources Sci. Technol., 10, 76 (2001).

Enhanced Global Model in Ar

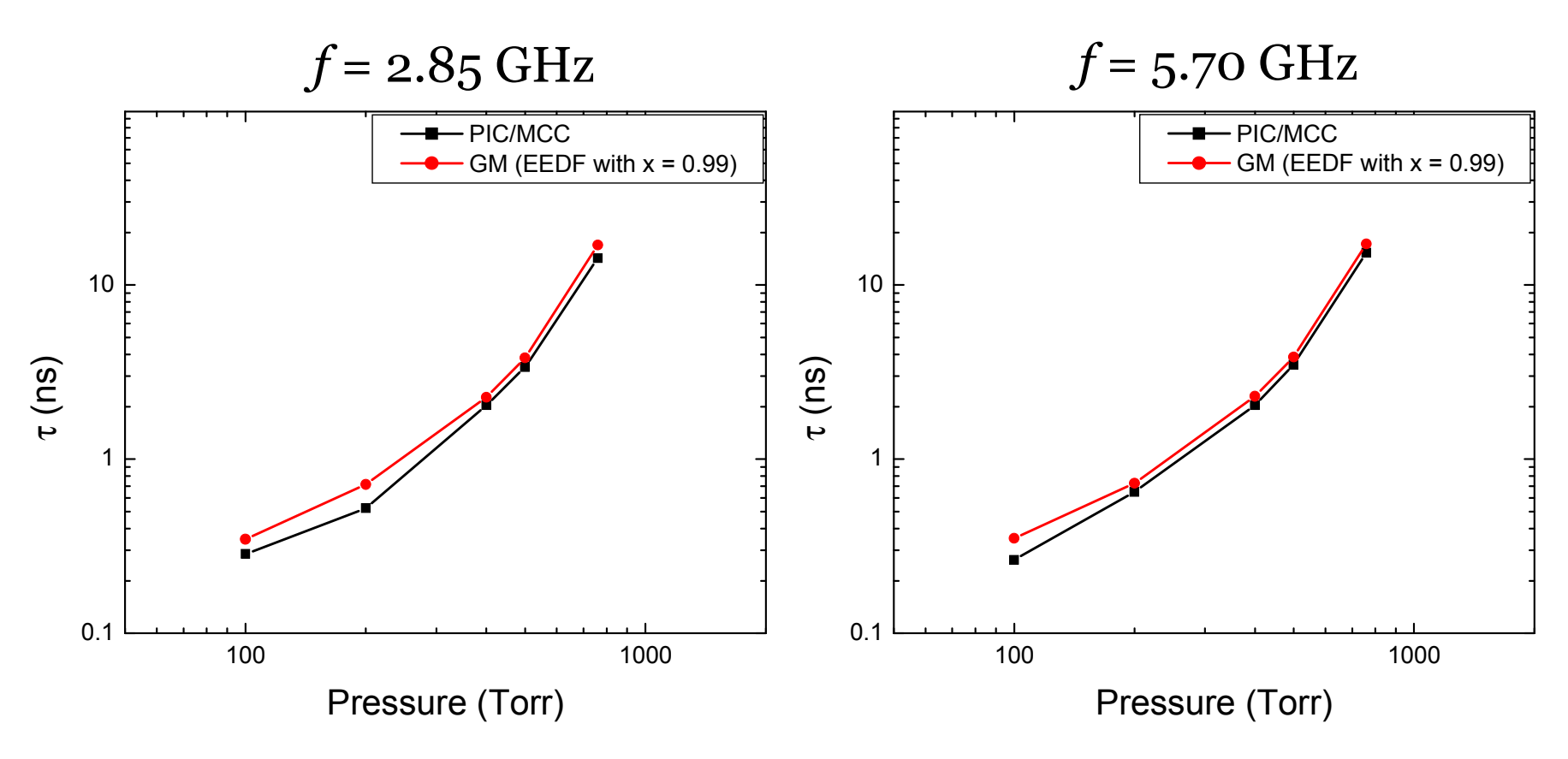




Breakdown Time in Air



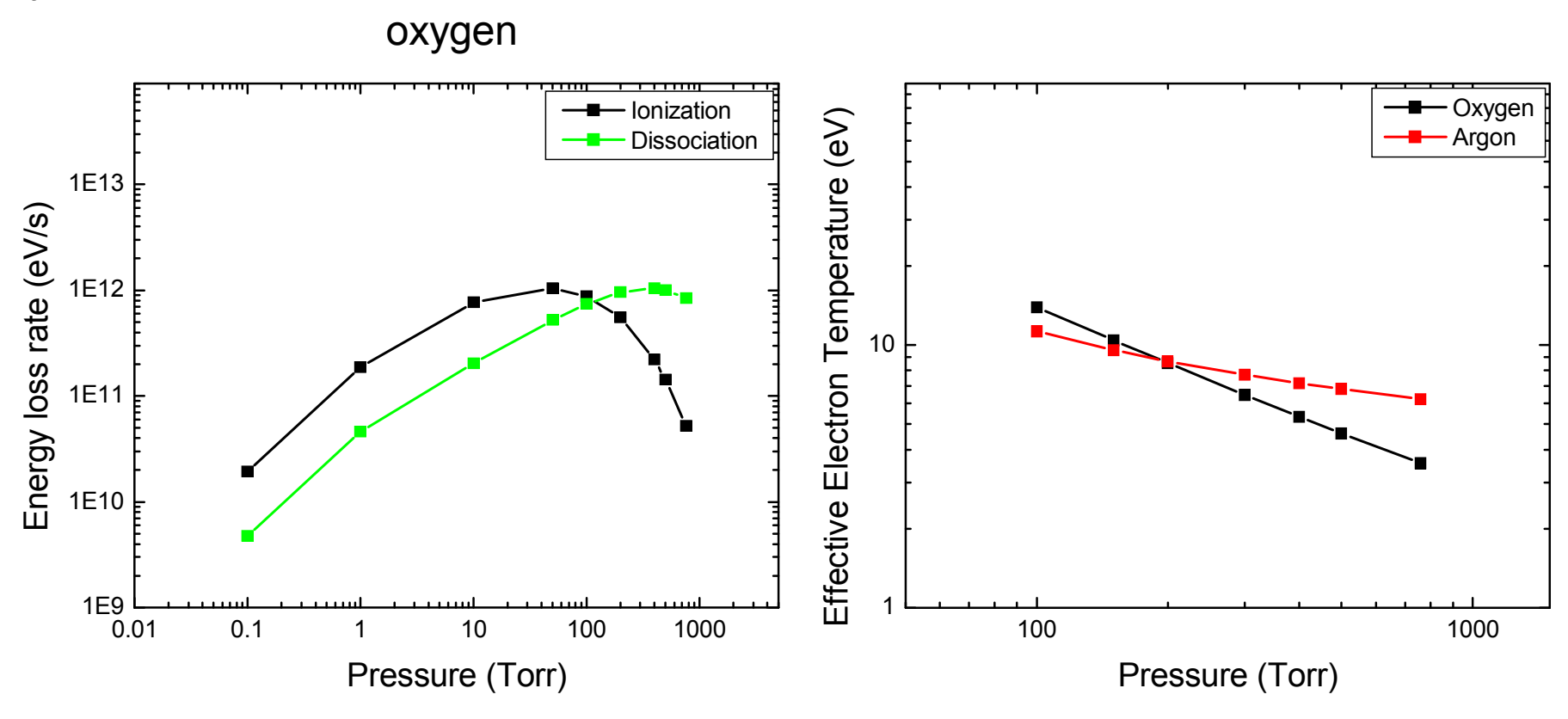
Air $E_0 = 4.23 \text{ MV/m}$



Energy loss rate and T_{eff}

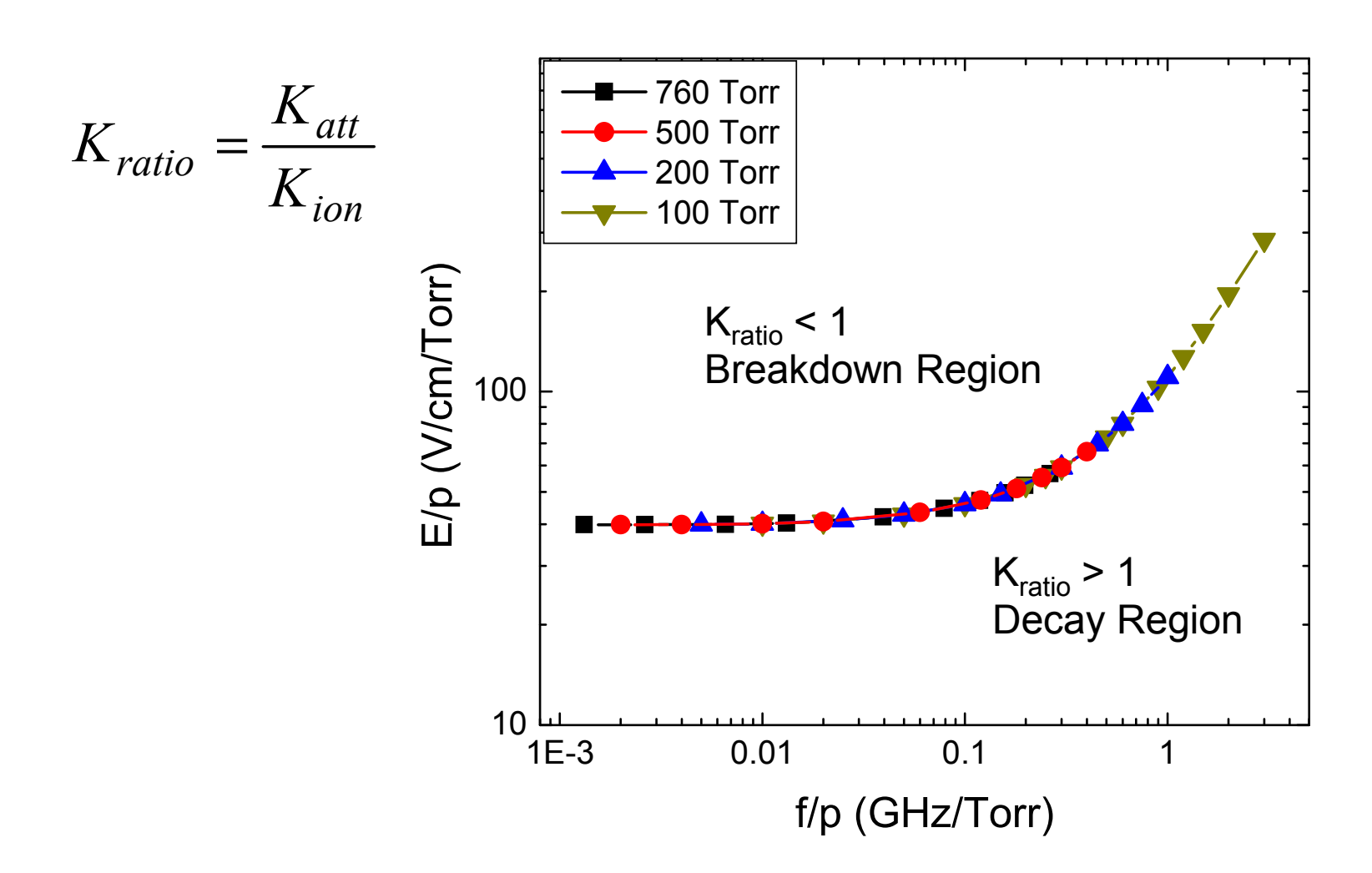


$$E_{\rm o}$$
 = 4.23 MV/m
 f = 2.85 GHz



Applied E vs f for K_{ratio} =1 in air





Effect of Frequency



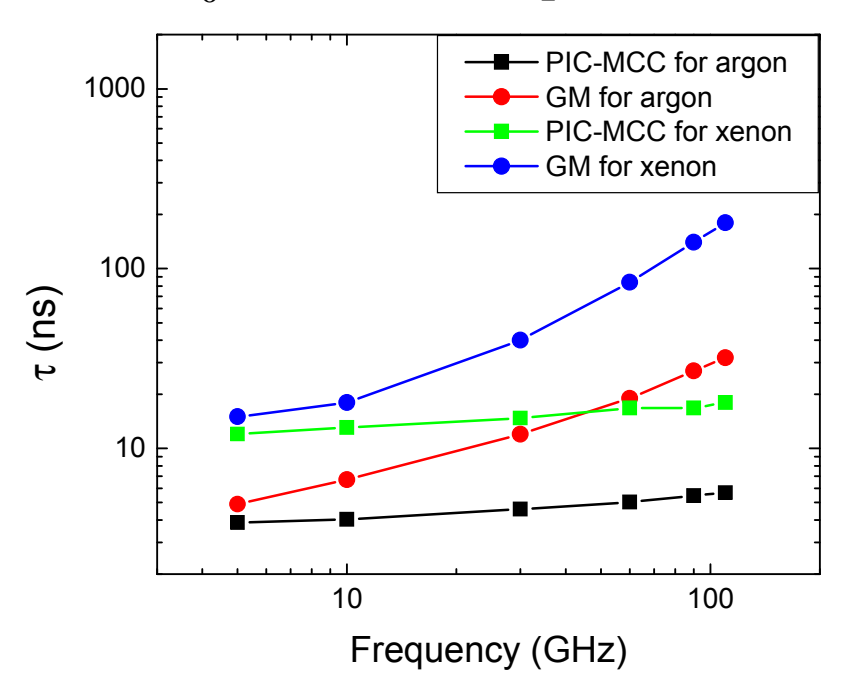
Constant x is inadequate at high frequency for Ramsauer gases

Argon

 $E_{\rm o}$ = 2.82 MV/m, p=500 Torr

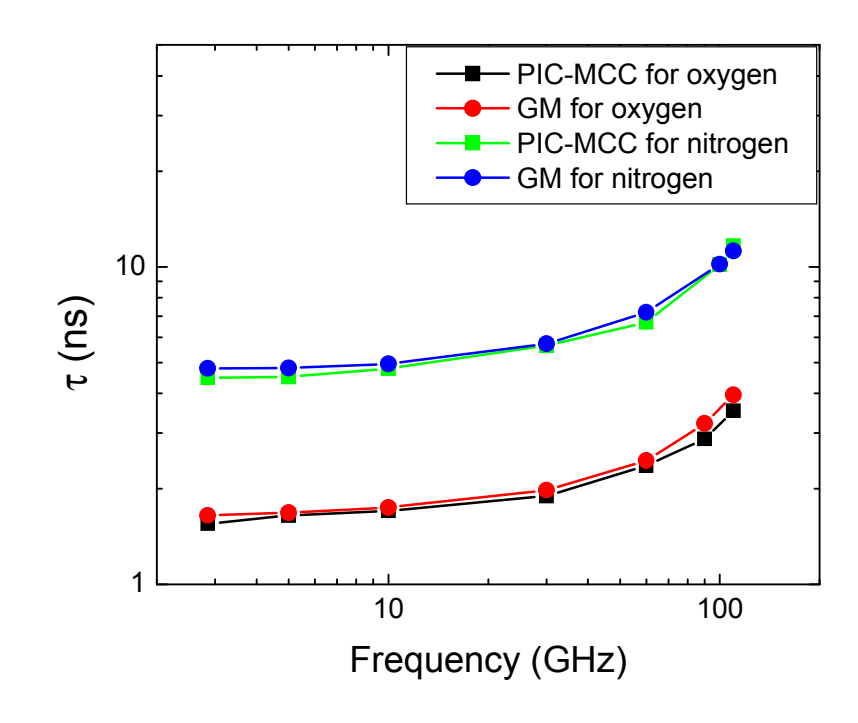
Xenon

$$E_0 = 2.82 \text{ MV/m}, p = 700 \text{ Torr}$$



Oxygen and Nitrogen

$$E_{\rm o}$$
 = 4.23 MV/m p = 500 Torr



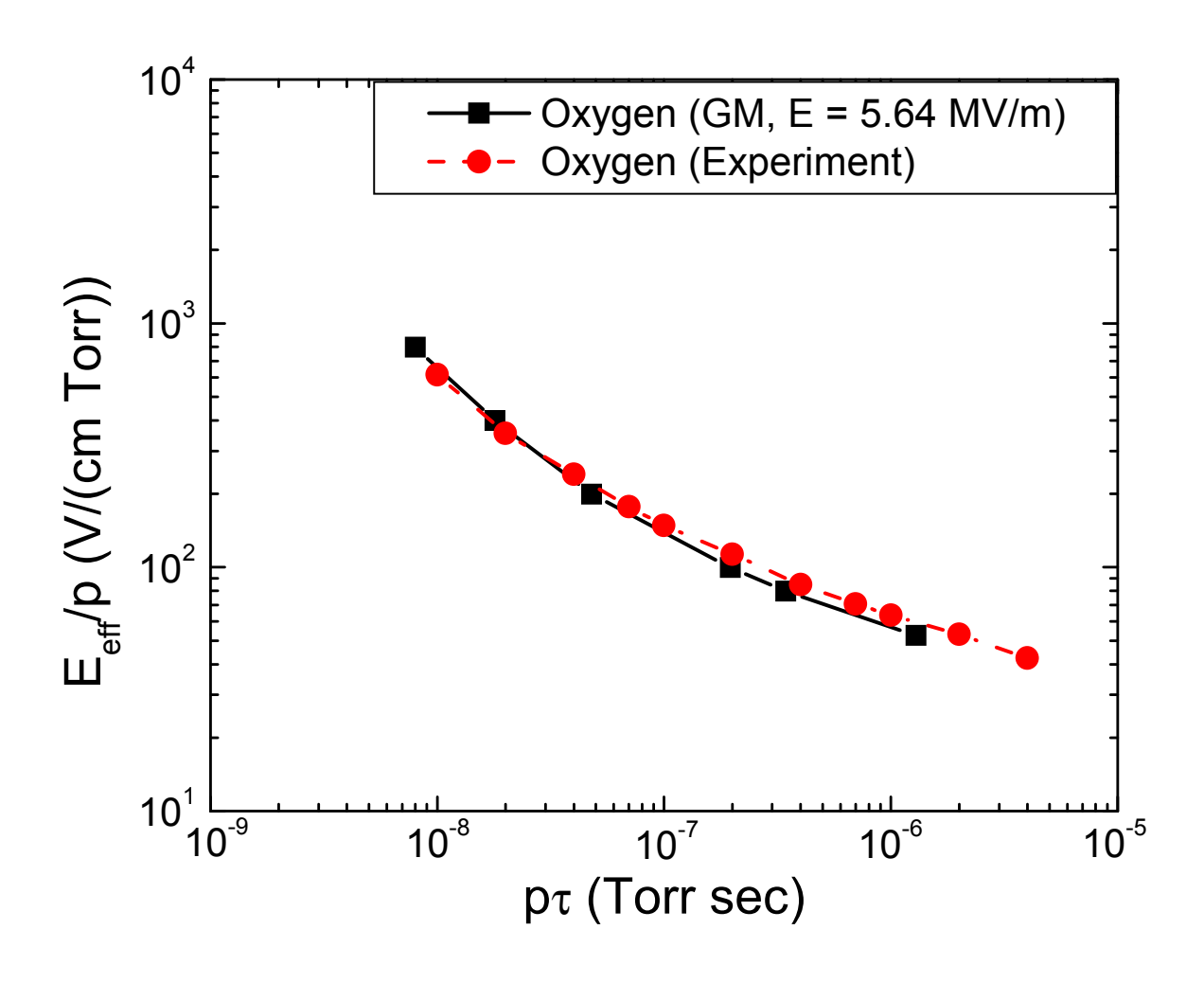
Sang Ki Nam and J. P. Verboncoeur, *Appl. Phys. Lett.*, **93**, 151504 (2008).

Argon: frequency dependence of x



Comparison to Experiment





^{*} P. Felsenthal and J. M. Proud, *Phys. Rev.*, **139**, A 1796 (1965).

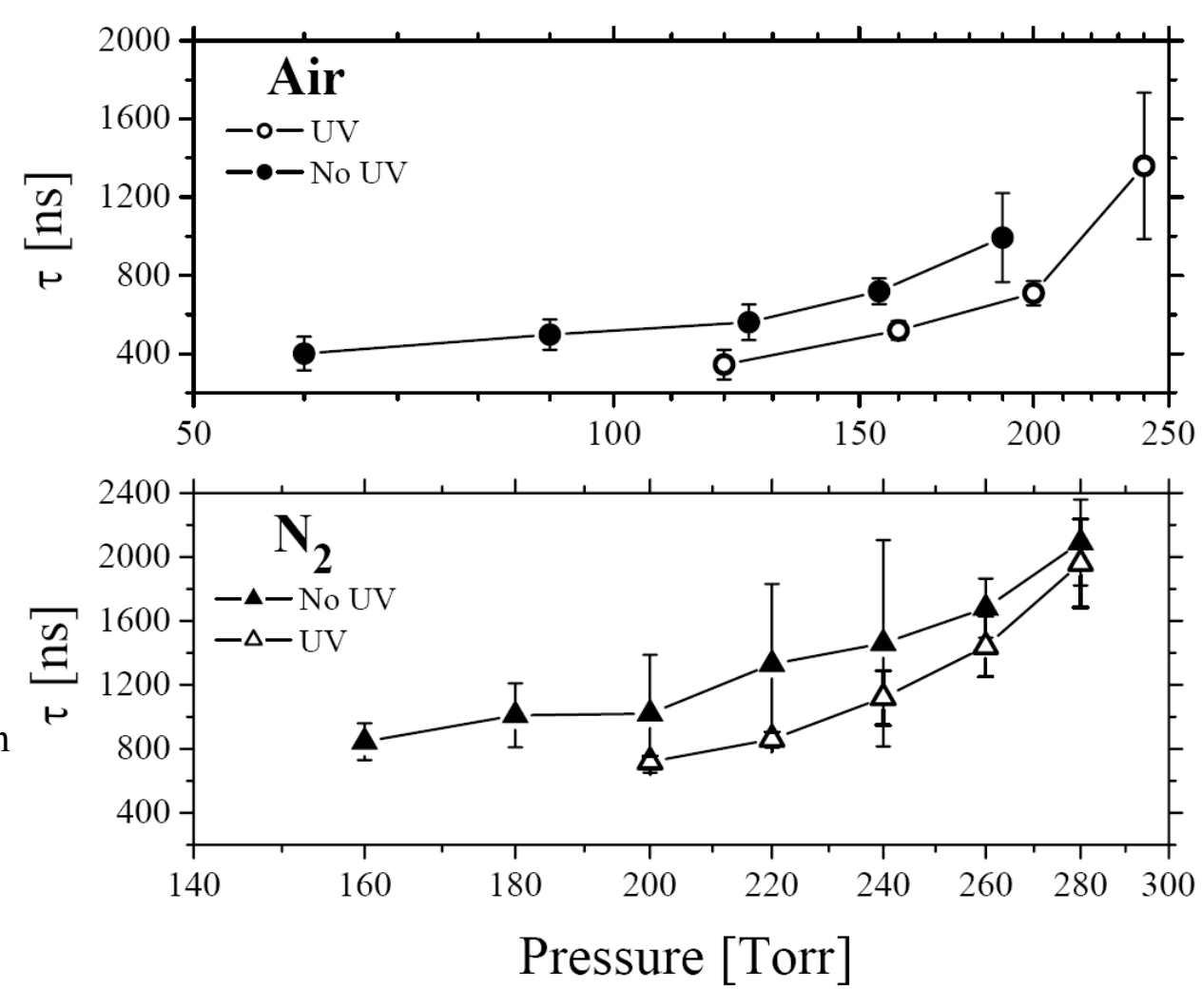


UV Illumination of Windows



Reduction in flashover delay time and standard deviation

- •4 MW, 2.5 μs incident pulse
- •Illumination intensity of approximately 4 mW/cm² over 240-400 nm range
- •Equivalent illumination of "sunny" day at 3000 ft. above sea level
- •Breakdown delay times exhibit less fluctuations with UV illumination
- •Sample-to-sample variance also somewhat reduced

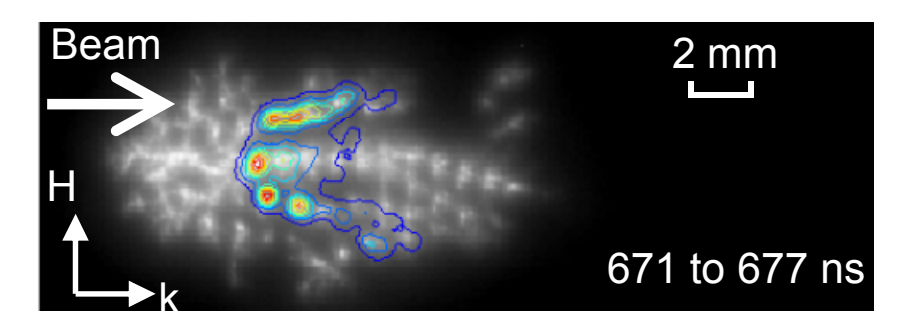




Plasma Filamentary Arrays



- 1.5 MW, 140 GHz Gyrotron
- 3 shots with slow (B&W) and fast (color) cameras
- Filaments spaced slightly less than $\lambda/4$, propagate towards source
- Hypothesis: constructive interference of reflected/diffracted waves, propagation speed limited by diffusion of seed electrons

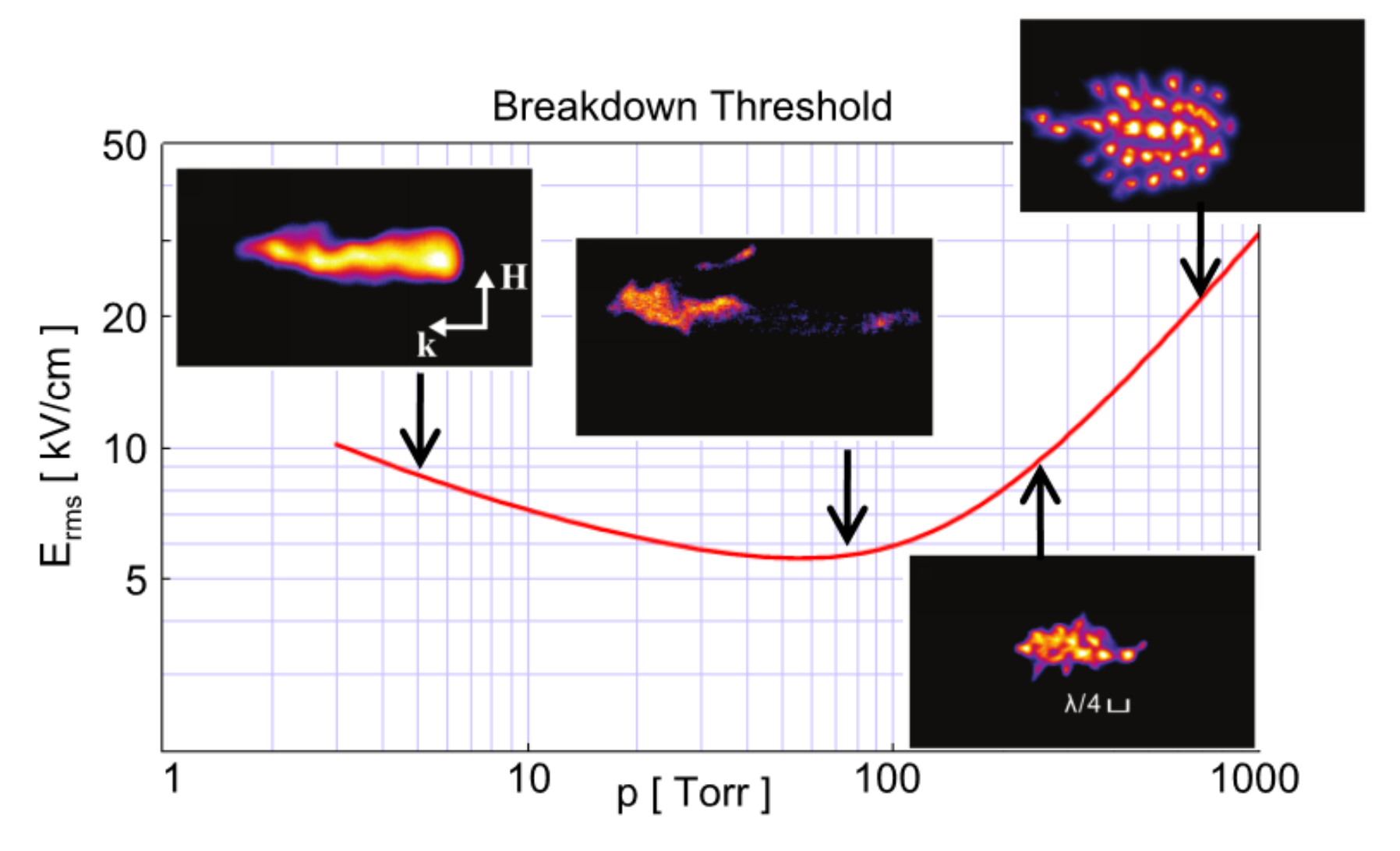






Pressure Dependence

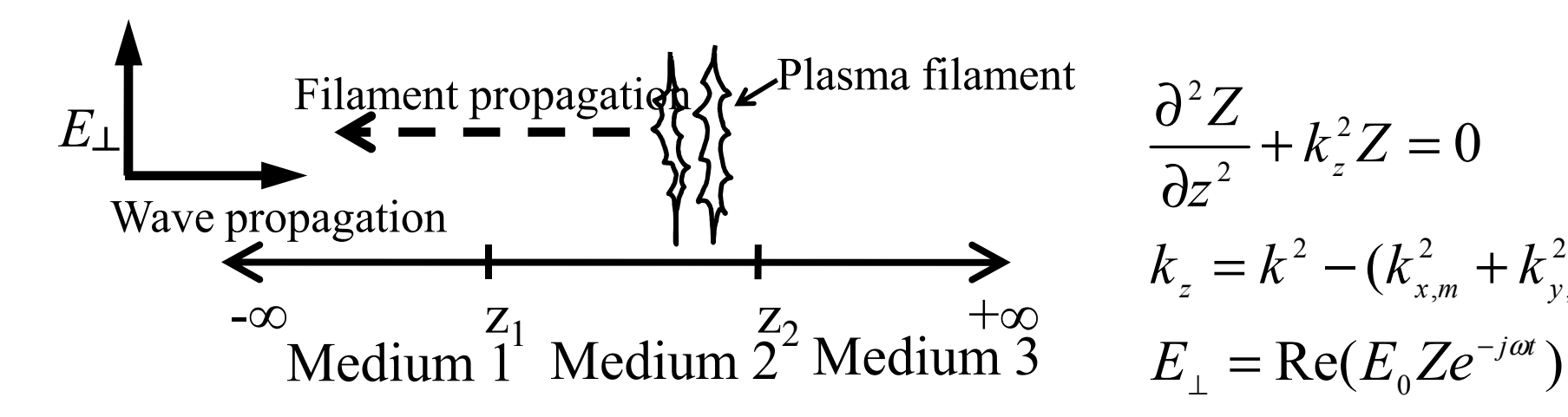




distinct filaments appear at high pressure

EM Wave Model





$$\frac{\partial^2 Z}{\partial z^2} + k_z^2 Z = 0$$

$$k_z = k^2 - (k_{x,m}^2 + k_{y,n}^2)$$

$$E_\perp = \text{Re}(E_0 Z e^{-j\omega t})$$

Z is spatial profile of E⊥

$$k_1^2 = k_3^2 = \frac{\alpha}{c}$$

$$k_{1}^{2} = k_{3}^{2} = \frac{\omega}{c}$$

$$k_{2}^{2} = \frac{\omega}{c} \left(1 - \sum_{i} \frac{\omega_{p,i}^{2}(z)}{\omega(\omega + j \nu_{m,i}(z))} \right)^{1/2}$$

 $\omega_{p,i}$: plasma frequency

 $V_{m,i}$: momentum transfer frequency

33

Fluid Model



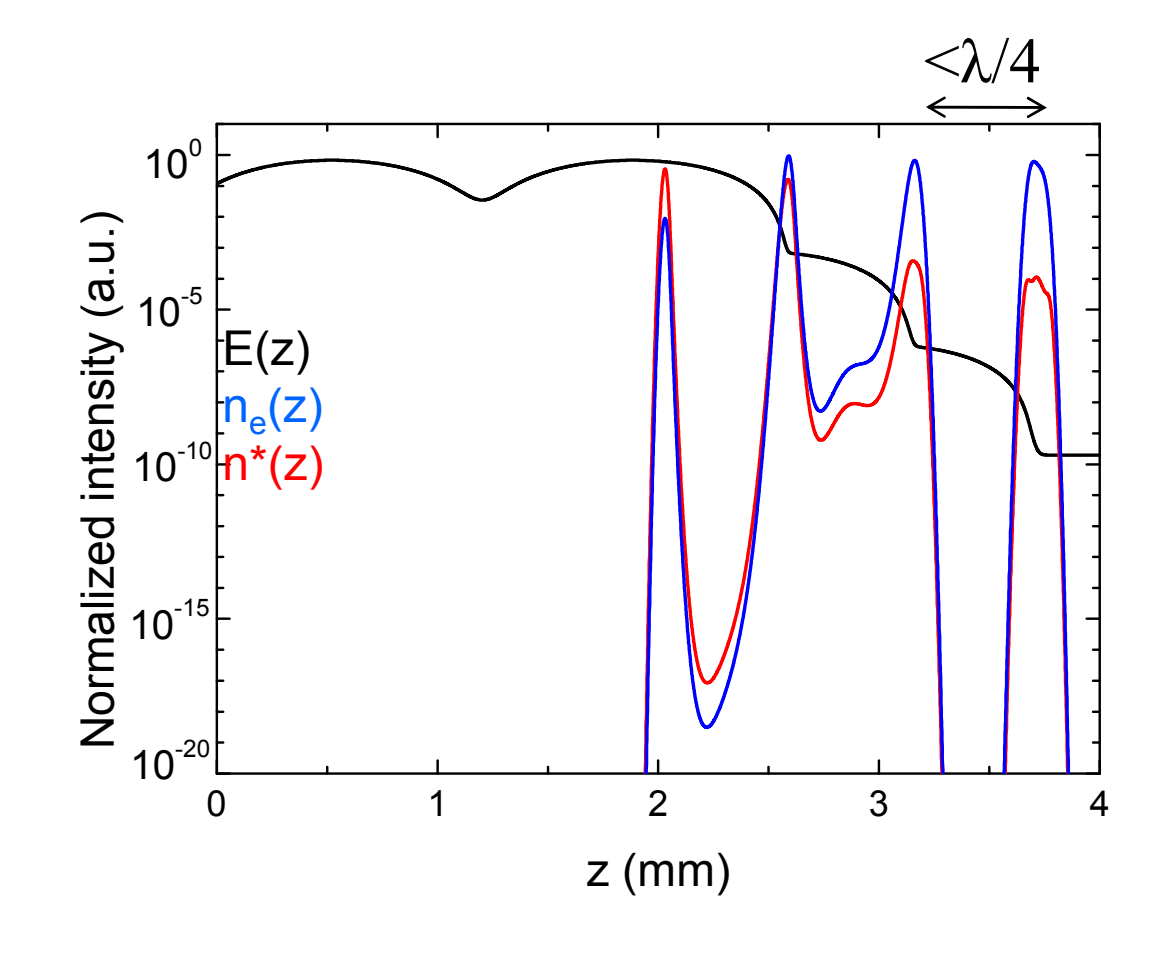
Particle Continuity and Electron Energy Equations

$$\begin{split} &\frac{\partial n_e}{\partial t} = -\nabla \cdot J_e + K_{ion} n_e n_{gas}, \ J_e = -D_e \nabla n_e - \mu_e n_e E_{\parallel} \\ &E_{\parallel} = \frac{D_i - D_e}{\mu_i + \mu_e} \frac{\nabla n_e}{n_e} \\ &\frac{\partial}{\partial t} \left(\frac{3}{2} n_e T_e \right) = -\nabla \cdot q_e + P_{abs} - (\varepsilon_{ion} K_{ion} n_e n_{gas} + \varepsilon_{exc} K_{exc} n_e n_{gas} + \widetilde{K}_{mom} n_e n_{gas}) \\ &q_e = -\frac{3}{2} D_e \nabla n_e T_e + \frac{5}{2} J_e T_e \\ &P_{abs} = \frac{e n_e}{m_e V_m} E_{\perp}^2 = \mu_e n_e E_{\perp}^2 \end{split}$$

Filaments: 1D Model



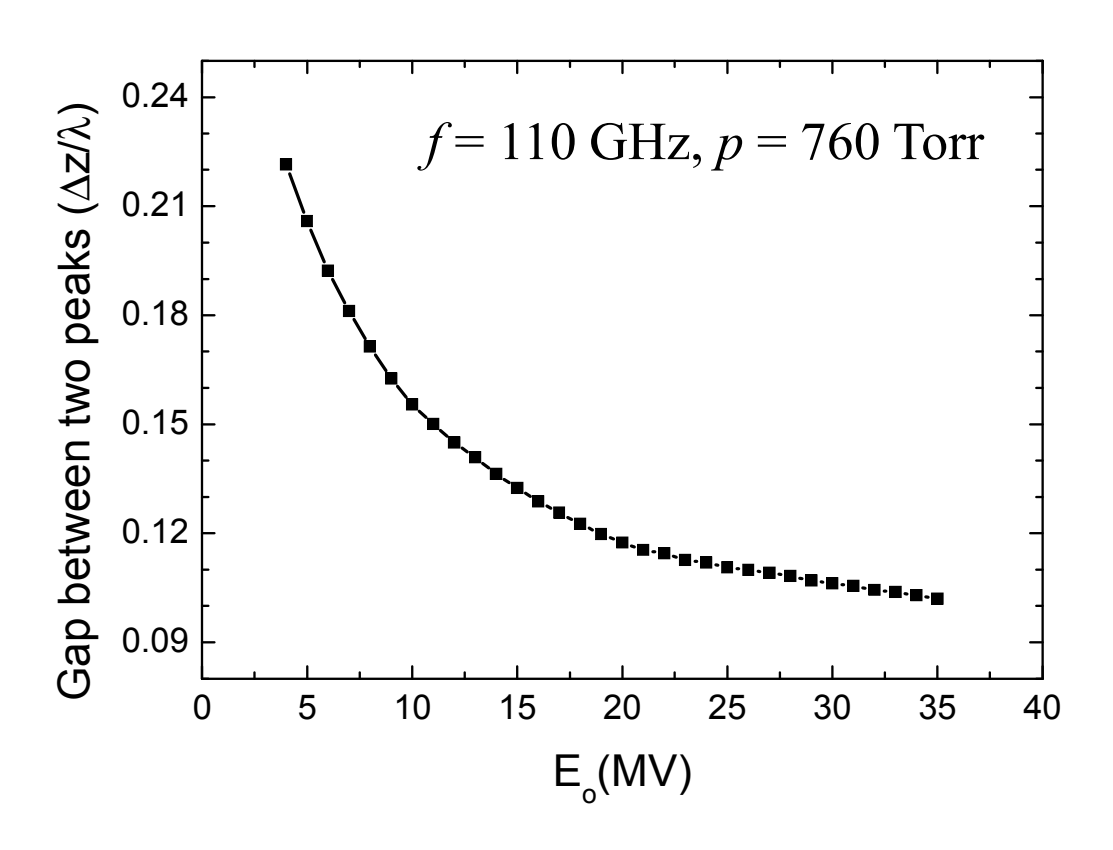
- Filaments propagate slowly toward source
- Explained via 1D fluid-EM model
- Ionization by electrons heated by EM absorption
- Standing waves via reflection
- Filament spacing depends on E, ω , gas



Kim et al., Comput. Phys. Comm. 177 (2007) Nam et al., Phys. Rev. Lett. 103 (2009)

Filament Spacing





Increasing field strength decreases filament spacing as breakdown threshold is exceeded closer to the previous filament.

Conclusions



- Modeling breakdown phenomena across a wide parameter regime
 - Multipactor dominates at low p
 - Multipactor and ionization discharge compete at intermediate pressure (10-50 Torr)
 - Ionization discharge dominates at atmospheric pressure
- Enhanced kinetic global model agrees with PIC model over 4 orders in pressure, 3 orders in f
 - EEDF shape nearly independent of p, E
 - EEDF shows some dependence on f for Ramsauer gases
- UV reduces statistical delay time
- Wave-fluid model reproduces filamentary experiment well
 - Filament distance slightly less than $\lambda/4$
 - Propagation speed ~ ambipolar or free diffusion times